NUMERICAL SIMULATIONS OF FUNDAMENTAL LIGHT-MATTER INTERACTIONS

Henry S. Qwabe

A dissertation submitted in fulfilment of the academic requirements for the degree of Masters of Science in the School of Chemistry and Physics, University of KwaZulu-Natal, Durban.

Supervisor:

Prof. Francesco Petruccione

Co-Supervisor:

Dr. Ilya Sinayskiy

December 2017

Contents

Abstract

We present the results of the numerical investigations of light-matter interactions in one and two dimensions from the quantum mechanical perspective. We investigate the dynamics of two-level systems coupled to quantized electromagnetic fields. We construct a quantum mechanical model to demonstrate how light interacts with classical objects such as mirrors and beam-splitters made from group of atoms, where each atom is modelled as a two-level system. We have been able to simulate behaviour of a single-photon being reflected and transmitted as a process of absorption and re-emission by the atoms.

Preface

The work reported in this dissertation was carried out in the School of Chemistry and Physics, University of KwaZulu-Natal, under the supervision of Prof. Francesco Petruccione and Dr. Ilya Sinayskiy.
As the candidate's supervisors we have approved this dissertation for submission.

Prof. F. Petruccione	Date
Dr. I. Sinayskiy	Date

Declaration - Plagiarism

I, Henry Simphiwe Qwabe declare that

1. The research reported in this thesis, except where otherwise indicated, is my original research.

2. This thesis has not been submitted for any degree or examination at any other university.

3. This thesis does not contain other persons' data, pictures, graphs or other information, unless specifically acknowledged as being sourced from other persons.

   (a) This thesis does not contain other persons' writing, unless specifically acknowledged as being sourced from other researchers. Where other written sources have been quoted, then:

   (b) Their words have been re-written but the general information attributed to them has been referenced; Where their exact words have been used, their writing has been placed inside quotation marks, and referenced.

4. This thesis does not contain text, graphics or tables copied and pasted from the Internet, unless specifically acknowledged, and the source being detailed in the thesis and in the References sections.

Signed: _____

Acknowledgement

I would like to express my deepest thanks to my supervisor Prof. Francesco Petruccione for support and guidance given to me through my MSc-studies. Alongside, I wish to thank my co-supervisor Dr. Ilya Sinayskiy for his constant guidance, providing all the necessary information and direction throughout my studies and making it possible. I would also like to give thanks to everyone (so as not to miss any names) in the Centre for Quantum Technology research group at the University of KwaZulu-Natal for all the help and motivation.

Chapter 1

Introduction

Quantum electrodynamics (QED) is an important building block of quantum field theory. QED is also better known as the quantum theory of light and has been seen as the most precise, if not, the most accurate and scientifically proven theory in the field of science at large [1, 2]. In essence, it explains how light and matter interact. Light has always been a subject of interest to humankind, it occupies a central role in the attempts to comprehend the nature in both quantum and classical mechanics. Most of the efforts have focused on the study of the generation of light and its applications in optical fibres and telecommunications. Light-matter interaction is one of the fundamental issues that remain of interest in the field of research and technological advancements. It is believed that, the interaction of light and matter forms a basis towards the understanding of almost every quantum platform that governs them. In general, the quantum theory of light, describes a system of direct interaction of photons and atoms, like cavity QED [3]. The study of matter at the atomic scale has been seen as one of the ambitious goals for the scientists in the past, present and future. Significant efforts have set the sight on implementing the strong coupling between photons and atoms [4–6]. Recent advances have shown some diverse methods on how one can manipulate single atoms with single photons [7, 8].

One of the famous approaches to light-matter interaction is the Jaynes-Cummings model which was proposed in 1963 by the two american physicists by the names of Edwin Jaynes and Fred Cummings [9]. This theoretical model was introduced to investigate the relation between quantum theory and the semi-classical theory of radiation, with the motivation to describe the process of spontaneous emission. Within

the process, they studied the interaction between an electromagnetic field mode and a quantum mechanical two-level system. Even though this model is undoubtedly an approximation, it plays an important role in understanding the fundamentals of light-matter interaction. This approach offers a quantum mechanical description of light-matter interaction that was in good agreement with experiments [10]. In addition, this model has induced a huge progress in the field of quantum optics and has become a fundamental principle in the field of quantum physics ever since. Over the past years, this model has been the core to further developments, which led to multiple applications and improvements like masers, lasers, optical trapping and cooling techniques, and more generally measuring and manipulating individual quantum systems (cavity QED)[10–12].

The main task of this work concerns the interactions between the atoms and the field at a fundamental level. This thesis presents the work based on an approach implemented in [13] which utilises the Jaynes-Cumming model. The basic idea of this numerical work is to regard the whole system to be in a quantum mechanical state. The authors of this paper outline how the results of several quantum mechanical simulations were conducted in the interaction picture. The aim of this thesis is to reproduce and improve the approach of this work. We study the dynamics of light interacting with matter with the help of numerical simulations. For this quantum mechanical model, light is described in terms of a single-photon wave packet created from a number of modes of electromagnetic radiation, whereas for the matter part, we are aiming to model optical elements such as mirrors and beam-splitters. These are modelled by an ensemble of two-level atoms [14, 15]. Usually, mirrors and beam-splitters are taken as classical objects that interact with the light. Classically, light being reflected by a mirror does not present any mystery. However, in this work, such light and mirror are ultimately described by photons and atoms. It is known that the process of reflection of light is quantum mechanical in nature. The interaction of light and matter is approximated by the Jaynes-Cummings model (building block of QED).

It is far from obvious how such a model ever explain the phenomenon of light reflection by a mirror. However, with the use of a two-dimensional cavity the authors of [13] were able to interpret the quantum behaviour of these optical components in the simulations. The state vector of the systems is taken to accept only a single ex-

citation. The field-atoms interaction is of the Jaynes-Cummings form, which ensures that the state vector keeps its single excitation. The authors of this paper then go on further and illustrate how to build quantum mirrors and beam-splitters using two-level atoms. The numerical analysis relies upon the use of the fast Fourier transform (FFT) to integrate the time evolution of the system.

The aim of this thesis is to implement numerical simulations of light-matter interactions on the fundamental level and extend the approach for future modelling of more complex experimental set-ups. The thesis is seen as the first step in the development of the numerical tools for the direct simulations of the light-matter interaction systems. Although it has been done already in [13], we are aiming in this thesis to familiarise ourselves with the technique and be able to reproduce what others have done. However, we want to try a slightly different approach. For our work we will conduct all the numerical simulations in the Schrödinger picture, and not in the interaction picture as previously demonstrated in [13]. In general, we consider a classical approach of how light and matter interact, then we transform that idea to work out a quantum mechanical description. In essence, we model a system of only one-photon interacting with a group of quantized atoms arranged into an atomic slab inside a two-dimensional cavity.

This thesis is structured in the following manner: In chapter 2, we give a brief quantum description of the atomic absorption and emission. We thereafter review the quantization of the electromagnetic field.

Chapter 3 is one of the key chapters. Here we further extend our discussion from the previous section in order to describe the model to work out the general Hamiltonians for the needs of the numerical simulations. Within the chapter, we look into the two-level approximation system. We illustrate how the calculations were derived. Lastly, we explain the numerical method that was adopted to conduct the simulations in 1-D and 2-D, respectively.

In chapter 4, we present the results of several simulations. We provide how a group of atoms can be used to build quantum mirrors and beam splitters for a system in 1-D and 2-D. Finally in chapter 5, we present the conclusion and a further discussion on possible extensions together with the applications of this work.

Chapter 2

Quantum mechanical description of an atom and quantization of the electromagnetic field

In this section, a description of an atom is explained by the classical electromagnetic radiation theory, or more precisely, by the quantum theory of light. In the next part of the present chapter, we study the quantization of the field. In essence, we describe the procedure by which quantum mechanics is applied to the electromagnetic field.

2.1 Quantum description of the atom

The focus of this thesis is the interaction of light with matter and thus, it is necessary for our work that we look into the details of this phenomena. For the basic understanding of matter, we are going to describe a simple two-level system that interacts with light. We consider a purely quantum-mechanical treatment to describe light-matter interactions in the presence of a two-level atomic system. In this work, atoms are modelled as two-level systems and they interact with light which is considered as a quantized electromagnetic field in a two-dimensional space. We assume that the energy level of the atoms and their positions are known. From the quantum-mechanical point of view, the position of the atoms are fixed by the interactions and by the Coulomb forces such that the atoms forms a crystal grid.
In the classical regime, it is well understood that the light which goes through any material is the same to that which comes out of it, governed by the laws of reflection

and refraction. However, the question that arises in the world of quantum physics is the following one. Can we say that the coherence properties of light remain the same after the reflection in the mirror or propagation through beam splitter? The process of reflection and transmission of the light by a material is the quantum-mechanical process of the re-absorption and re-emission. In essence, does the light that is being absorbed by the material as a form of light interacting with the quantum matter remain the same after reflection? Our intention is to show that, because all the experimental observations proves that the light has to be the same then one can take this kind of classical optics laws and transform it to quantum mechanics. The ability of the computational techniques allows us to implement these theoretical demonstrations. Therefore, it turns out that an atom has the ability to absorb and to emit the light. By the understanding of the quantum hypothesis that energy exists in little packets of certain sizes then one can better understand the process by which atoms absorb and emit the light [1]. In 1913 Niels Bohr proposed a theory that explains how a quantum light of frequency ω is either absorbed or emitted when an atomic transition occurs between the two quantized energy levels that fulfil the following relation:

$$E_2 - E_1 = \hbar\omega, \tag{2.1}$$

where E_1 and E_2 represents the lower and upper energy levels. It became traditional in many theoretical treatments to present an atom in any quantum system with two-eigenstates respectively [16]. Since then, this theory was further developed by Einstein who introduced what is known as Einstein coefficients to indicate how the quantum light undergoes the process of absorption and re-emission by atoms. It is well understood that every atom is made up of a nucleus together with one or more electrons which are bound to the nucleus itself. In Fig. 2.1 we show the process of absorption and re-emission which happens as a result of light-atoms interaction in the field of quantum physics. Within Fig. 2.1, there are two diagrams. Part (a) illustrates the absorption and part (b) the re-emission of the photon by atoms. In both diagrams we have two energy levels with an atom and photon ($\hbar\omega$) shown by a wave arrow which gives us an idea that a photon is light and that light has a wave nature. Let us consider first the absorption process in Fig. 2.1(a). Let us assume that, the atom is initially lying in the lower energy level E_1 and the photon comes in. The atom will absorb the photon. The atom will gain the energy of the photon, then it will eventually jump to

(a) (b)

Figure 2.1: Optical transitions between the quantized energy levels: (a) absorption, and (b) re-emission processes.

the higher energy level E_2, also known as the excited state. Similarly, the re-emission process is shown in Fig. 2.1(b). Here, the atom is in the upper energy level, but the moment the atom emits the photon the atom now drops back down to the lower energy level E_1, also known as the ground state. So basically, in the event of photon emission the atom loses some of the energy.

2.2 Solutions to the classical Maxwell's equations for the electromagnetic field waves in a box at the pre-condition for the quantization

The main objective in this section is to review the classical and quantum mechanical properties of the electromagnetic field. We begin by quantizing the classical electromagnetic field which is described by a set of four equations named after J. C. Maxwell [17]. These Maxwell equations explain several phenomena related to the electric and magnetic fields. Let us consider a classical electromagnetic field in an empty space, assuming that there are no sources like charges and currents present. The field fulfils

these homogeneous Maxwell equations which in SI units reads as

$$\nabla \times \mathbf{E}(\mathbf{r},t) = -\frac{\partial \mathbf{B}(\mathbf{r},t)}{\partial t}, \tag{2.2}$$

$$\nabla \times \mathbf{B}(\mathbf{r},t) = \frac{1}{c^2}\frac{\partial \mathbf{E}(\mathbf{r},t)}{\partial t}, \tag{2.3}$$

$$\nabla \cdot \mathbf{E}(\mathbf{r},t) = 0, \tag{2.4}$$

$$\nabla \cdot \mathbf{B}(\mathbf{r},t) = 0, \tag{2.5}$$

where c is the speed of light in vacuum and $\mathbf{E}(\mathbf{r},t)$, $\mathbf{B}(\mathbf{r},t)$ denotes the electric and magnetic field, respectively. In general, it is more convenient to let the free electromagnetic field be represented by the transverse vector potential $\mathbf{A}(\mathbf{r},t)$ in the Coulomb gauge such that it fulfils the homogeneous wave equation,

$$\nabla^2 \mathbf{A}(\mathbf{r},t) - \frac{1}{c^2}\frac{\partial^2}{\partial t^2}\mathbf{A}(\mathbf{r},t) = 0, \tag{2.6}$$

where operator ∇^2 is the Laplacian and the divergence condition

$$\nabla \cdot \mathbf{A}(\mathbf{r},t) = 0. \tag{2.7}$$

We can define the electric and magnetic fields $\mathbf{E}(\mathbf{r},t)$ and $\mathbf{B}(\mathbf{r},t)$ in terms of the vector potential $\mathbf{A}(\mathbf{r},t)$ in the following way

$$\mathbf{E}(\mathbf{r},t) = -\frac{\partial}{\partial t}\mathbf{A}(\mathbf{r},t), \tag{2.8}$$

$$\mathbf{B}(\mathbf{r},t) = \nabla \times \mathbf{A}(\mathbf{r},t). \tag{2.9}$$

In order for us to determine the Hamiltonian equations of motion, it is better that we first consider a Fourier decomposition of the vector potential $\mathbf{A}(\mathbf{r},t)$ with respect to its space variables x, y, z. This can be achieved as either in the form of a Fourier integral or as of a Fourier series. There is no clear advantage between these two forms at this

stage, however, we will find it straightforward to deal with the quantized field in terms of a discrete decomposition of $\mathbf{A}(\mathbf{r},t)$. Thus, we assume that the electromagnetic field is contained in a very large cube of side L and set the periodic boundary conditions on the field. At some point in the calculations, we will allow L to tend to infinity. As might be expected, any physically meaningful result must not be controlled by the magnitude of side of the cube L. Let us consider the three-dimensional Fourier expansion of vector potential $\mathbf{A}(\mathbf{r},t)$ in terms of a plane-wave mode to have the form

$$\mathbf{A}(\mathbf{r},t) = \frac{1}{\varepsilon_0^{1/2} L^{3/2}} \sum_{\mathbf{k}} \mathscr{A}_{\mathbf{k}}(t) \exp(i\mathbf{k}\cdot\mathbf{r}), \tag{2.10}$$

where terms ε_0 denotes vacuum dielectric constant and $\mathscr{A}_{\mathbf{k}}(t)$ is the coefficient of the Fourier expansion of $\mathbf{A}(\mathbf{r},t)$, respectively. The wave vector $\mathbf{k}$ has the components

$$\begin{aligned} k_1 =& \frac{2\pi}{L} n_1, \qquad n_1 = 0, \pm 1, \pm 2, ... \\ k_2 =& \frac{2\pi}{L} n_2, \qquad n_2 = 0, \pm 1, \pm 2, ... \\ k_3 =& \frac{2\pi}{L} n_3. \qquad n_3 = 0, \pm 1, \pm 2, ... \end{aligned} \tag{2.11}$$

They form a discrete set, and the summation $\sum_{\mathbf{k}}$ represents the sum over the integers n_1, n_2, and n_3. When we apply the Coulomb gauge in Eq. (2.7) to the plane wave with the periodic boundary condition in sight of the transversality condition we get that

$$\frac{i}{\varepsilon_0^{1/2} L^{3/2}} \sum_{\mathbf{k}} \mathbf{k}\cdot\mathscr{A}_{\mathbf{k}}(t) \exp(i\mathbf{k}\cdot\mathbf{r}) = 0, \tag{2.12}$$

for all $\mathbf{r}$, such that

$$\mathbf{k}\cdot\mathscr{A}_{\mathbf{k}}(t) = 0. \tag{2.13}$$

Furthermore, the physical existence of $\mathbf{A}(\mathbf{r},t)$ leads us to the following condition

$$\mathscr{A}_{-\mathbf{k}}(t) = \mathscr{A}^*_{\mathbf{k}}(t). \tag{2.14}$$

Since the vector potential $\mathbf{A}(\mathbf{r},t)$ fulfils the homogeneous wave equation in Eq. (2.6), this implies that

$$\frac{1}{\varepsilon_0^{1/2}L^{3/2}}\sum_{\mathbf{k}}\left(-k^2-\frac{1}{c^2}\frac{\partial^2}{\partial t^2}\right)\mathscr{A}_{\mathbf{k}}(t)\exp(i\mathbf{k}\cdot\mathbf{r})=0 \tag{2.15}$$

for all $\mathbf{r}$, such that $\mathscr{A}_{\mathbf{k}}(t)$ fulfils the following equation of of motion

$$\left(\frac{\partial^2}{\partial t^2}+\omega_{\mathbf{k}}^2\right)\mathscr{A}_{\mathbf{k}}(t)=0. \tag{2.16}$$

In Eq. (2.16), we introduced the angular frequency $\omega_{\mathbf{k}}=ck$. The general solution to Eq. (2.16), which also happens to obey the condition in Eq. (2.14) is given as

$$\mathscr{A}_{\mathbf{k}}(t)=\mathbf{c}_{\mathbf{k}}\exp(-i\omega_{\mathbf{k}}t)+\mathbf{c}_{-\mathbf{k}}^{*}\exp(i\omega_{\mathbf{k}}t). \tag{2.17}$$

It is important for us that we work out the vector $\mathbf{c}_{\mathbf{k}}$ into two orthogonal components, which are chosen such that they satisfy the condition given by Eq. (2.13). This can be achieved by the means of selecting a pair of orthonormal polarisation vectors $\varepsilon_{\mathbf{k}1}$, $\varepsilon_{\mathbf{k}2}$ which obey the following conditions

$$\begin{aligned}\mathbf{k}\cdot\varepsilon_{\mathbf{k}s}&=0, \qquad (s=1,2)\\ \varepsilon_{\mathbf{k}s}^{*}\cdot\varepsilon_{\mathbf{k}s'}&=\delta_{ss'}, \qquad (s,s'=1,2)\\ \varepsilon_{\mathbf{k}1}\times\varepsilon_{\mathbf{k}2}&=\mathbf{k}/k\equiv\kappa,\end{aligned} \tag{2.18}$$

which indicate then transversality, orthonormality and the right-handedness respectively. We now define the vector $\mathbf{c}_{\mathbf{k}}$ to be

$$\mathbf{c}_{\mathbf{k}}=\sum_{s=1}^{2}c_{\mathbf{k}s}\varepsilon_{\mathbf{k}s}. \tag{2.19}$$

The complex conjugate in line two from Eq. (2.18) is not needed, provided the $\varepsilon_{\mathbf{k}s}$ are real. The two real base vectors $\varepsilon_{\mathbf{k}1}$, $\varepsilon_{\mathbf{k}2}$ amount to the two states of orthogonal linear polarization. The vector $\mathbf{c}_{\mathbf{k}}$ in Eq. (2.19) corresponds to the resolution of the field amplitude into two orthogonal linear polarizations. The conditions that were selected in Eq. (2.18) on the two base vectors does not determine them, but rather leaves them undefined up to a rotation about the wave vector $\mathbf{k}$.

While the expansion in Eq. (2.19) is understood to be rational regardless of which base vectors $\varepsilon_{\mathbf{k}s}$ are taken, in general it is more convenient to leave them undefined in the analysis, pending that we reach a stage when it becomes clear enough that one particular set of base vectors simplifies the calculation. Thus, the base vectors at that stage can be chosen in a manner that is suitable. We substitute Eq. (2.19) into Eq. (2.17) and then make use of the results in Eq. (2.10). This leads us to the expansion of the form

$$\begin{aligned}\mathbf{A}(\mathbf{r},t) =& \frac{1}{\varepsilon_0^{1/2}L^{3/2}}\sum_{\mathbf{k}}\sum_{s=1}^{2}[c_{\mathbf{k}s}\varepsilon_{\mathbf{k}s}\exp(-i\omega_{\mathbf{k}s}t)+c^*_{-\mathbf{k}s}\varepsilon^*_{-\mathbf{k}s}\exp(i\omega_{\mathbf{k}s}t)]\exp(i\mathbf{k}\cdot\mathbf{r})\\ =& \frac{1}{\varepsilon_0^{1/2}L^{3/2}}\sum_{\mathbf{k}}\sum_{s=1}^{2}[c_{\mathbf{k}s}\varepsilon_{\mathbf{k}s}\exp[i(\mathbf{k}\cdot\mathbf{r}-\omega_{\mathbf{k}s}t)]+c^*_{\mathbf{k}s}\varepsilon^*_{\mathbf{k}s}\exp -i[(\mathbf{k}\cdot\mathbf{r}-\omega_{\mathbf{k}s}t)]]\\ =& \frac{1}{\varepsilon_0^{1/2}L^{3/2}}\sum_{\mathbf{k}}\sum_{s=1}^{2}[u_{\mathbf{k}s}(t)\varepsilon_{\mathbf{k}s}\exp(i\mathbf{k}\cdot\mathbf{r})+u^*_{\mathbf{k}s}(t)\varepsilon^*_{\mathbf{k}s}\exp(-i\mathbf{k}\cdot\mathbf{r})],\end{aligned} \tag{2.20}$$

where we have let

$$u_{\mathbf{k}s}(t) = c_{\mathbf{k}s}\exp(-i\omega_{\mathbf{k}s}t). \tag{2.21}$$

Therefore, Eq. (2.20) is regarded as the expansion of the vector potential $\mathbf{A}(\mathbf{r},t)$ in terms of the fundamental vector mode functions $\varepsilon_{\mathbf{k}s}\exp(i\mathbf{k}\cdot\mathbf{r})$, with the complex amplitudes given in Eq. (2.21) respectively. We label each mode by a wave vector $\mathbf{k}$ together with the polarization index s. Essentially, the corresponding mode function clearly fulfils the Helmholtz equation such that

$$(\nabla^2+k^2)\varepsilon_{\mathbf{k}s}\exp(i\mathbf{k}\cdot\mathbf{r}) = 0, \tag{2.22}$$

whereas the corresponding mode amplitude $u_{\mathbf{k}s}(t)$ also fulfils the same harmonic oscillator equation of motion in Eq. (2.16) as $\mathscr{A}_{\mathbf{k}}(t)$. One can utilize the relation in Eq. (2.20) to obtain the mode expansions for the electric and magnetic fields $\mathbf{E}(\mathbf{r},t)$ and $\mathbf{B}(\mathbf{r},t)$ given the expressions in Eq. (2.8), Eq. (2.9). Hence

$$\mathbf{E}(\mathbf{r},t) = \frac{i}{\varepsilon_0^{1/2}L^{3/2}}\sum_{\mathbf{k}}\sum_{s=1}^{2}\omega_{\mathbf{k}s}[u_{\mathbf{k}s}(t)\varepsilon_{\mathbf{k}s}\exp(i\mathbf{k}\cdot\mathbf{r})-\text{c.c}], \tag{2.23}$$

and

$$\mathbf{B}(\mathbf{r},t) = \frac{i}{\varepsilon_0^{1/2} L^{3/2}} \sum_{\mathbf{k}} \sum_{s=1}^{2} [u_{\mathbf{k}s}(t)(\mathbf{k} \times \varepsilon_{\mathbf{k}s}) \exp(i\mathbf{k} \cdot \mathbf{r}) - \text{c.c}]. \tag{2.24}$$

Let us consider Eq. (2.23) and Eq. (2.24) in order to work out the energy H of the field, which we call the Hamiltonian function and has the form

$$\mathcal{H} = \frac{1}{2} \int_{L^3} [\varepsilon_0 \mathbf{E}^2(\mathbf{r},t) + \frac{1}{\mu_0} \mathbf{B}^2(\mathbf{r},t)] d^3r. \tag{2.25}$$

The energy of the field is given by the integral over the volume of the box L^3. If we substitute $\mathbf{E}(\mathbf{r},t)$ and $\mathbf{B}(\mathbf{r},t)$ back into Eq. (2.25) and then carry out the integration over the space contained with the support from the following relations

$$\begin{aligned} \int_{L^3} \exp[i(\mathbf{k} - \mathbf{k}') \cdot \mathbf{r}] d^3r =& L^3 \delta^3_{\mathbf{k}\mathbf{k}'}, \\ (\mathbf{k} \times \varepsilon^*_{-\mathbf{k}s}) \cdot (\mathbf{k} \times \varepsilon_{\mathbf{k}s'}) =& k^2 \varepsilon^*_{\mathbf{k}s} \cdot \varepsilon_{\mathbf{k}s'} = k^2 \delta_{ss'}, \end{aligned} \tag{2.26}$$

we get the following classical Hamiltonian expression

$$\mathcal{H} = 2 \sum_{\mathbf{k}} \sum_{s=1}^{2} \omega^2_{\mathbf{k}s} |\ u_{\mathbf{k}s}(t)|^2, \tag{2.27}$$

which illustrates the energy as a sum over the modes. Since our intention is to quantize the field, it is necessary that we re-write H in the Hamiltonian form. This can be done by introducing a set of real canonical variables $q_{\mathbf{k}s}$ and $p_{\mathbf{k}s}$ as

$$q_{\mathbf{k}s} = [u_{\mathbf{k}s}(t) + u^*_{\mathbf{k}s}(t)], \tag{2.28}$$

$$p_{\mathbf{k}s} = -\, i\omega_{\mathbf{k}s} [u_{\mathbf{k}s}(t) - u^*_{\mathbf{k}s}(t)]. \tag{2.29}$$

Taking into consideration the time dependence of $u_{\mathbf{k}s}(t)$ given in Eq. (2.21), the two variables $q_{\mathbf{k}s}(t)$ and $p_{\mathbf{k}s}(t)$ oscillate sinusoidally in time (t) at the frequency ω, and

usually we get the following relations

$$\frac{\partial}{\partial t} q_{\mathbf{k}s}(t) = p_{\mathbf{k}s}(t), \tag{2.30}$$

$$\frac{\partial}{\partial t} p_{\mathbf{k}s}(t) = -\omega_{\mathbf{k}s}^2 q_{\mathbf{k}s}(t). \tag{2.31}$$

We can re-write the expression in Eq. (2.27) for the classical Hamiltonian in terms of the $q_{\mathbf{k}s}(t)$ and $p_{\mathbf{k}s}(t)$ as follows

$$\mathcal{H} = \frac{1}{2} \sum_{\mathbf{k}} \sum_{s=1}^{2} [p_{\mathbf{k}s}^2(t) + \omega_{\mathbf{k}s}^2 q_{\mathbf{k}s}^2(t)]. \tag{2.32}$$

This expression is seen as the energy of a system of independent harmonic oscillators. Each harmonic oscillator corresponds to a single mode of the electromagnetic field described by the wave vector $\mathbf{k}$ and state of polarisation s. The set of all canonical variables $q_{\mathbf{k}s}(t)$, $p_{\mathbf{k}s}(t)$ describes the state of the classical radiation field. The set is understood to be infinite, however due to the fact that we are dealing with the finite volume together with the discrete set of modes, it is countably infinite. Let us consider the canonical equations of motion in terms of the canonical variables to be

$$\frac{\partial \mathcal{H}}{\partial p_{\mathbf{k}s}} = \frac{\partial q_{\mathbf{k}s}}{\partial t}, \tag{2.33}$$

and

$$\frac{\partial \mathcal{H}}{\partial q_{\mathbf{k}s}} = -\frac{\partial p_{\mathbf{k}s}}{\partial t}. \tag{2.34}$$

These expressions are similar to those in Eqs. (2.30) and (2.31) respectively. The expansions in Eqs. (2.20), (2.23) and (2.24) for the field vectors $\mathbf{A}(\mathbf{r}, t)$, $\mathbf{E}(\mathbf{r}, t)$, $\mathbf{B}(\mathbf{r}, t)$

can be expressed in terms of the canonical variables as

$$\mathbf{A}(\mathbf{r},t) = \frac{1}{\varepsilon_0^{1/2} L^{3/2}} \sum_{\mathbf{k}} \sum_{s=1}^{2} \{[q_{\mathbf{k}s}(t) + \frac{i}{\omega_{\mathbf{k}s}} p_{\mathbf{k}s}(t)] \varepsilon_{\mathbf{k}s} \exp(i\mathbf{k}\cdot\mathbf{r}) + \text{c.c}\}, \tag{2.35}$$

$$\mathbf{E}(\mathbf{r},t) = \frac{i}{\varepsilon_0^{1/2} L^{3/2}} \sum_{\mathbf{k}} \sum_{s=1}^{2} \{[\omega_{\mathbf{k}s} q_{\mathbf{k}s}(t) + i p_{\mathbf{k}s}(t)] \varepsilon_{\mathbf{k}s} \exp(i\mathbf{k}\cdot\mathbf{r}) - \text{c.c}\}, \tag{2.36}$$

$$\mathbf{B}(\mathbf{r},t) = \frac{i}{\varepsilon_0^{1/2} L^{3/2}} \sum_{\mathbf{k}} \sum_{s=1}^{2} \{[q_{\mathbf{k}s}(t) + \frac{i}{\omega_{\mathbf{k}s}} p_{\mathbf{k}s}(t)] \mathbf{k} \times \varepsilon_{\mathbf{k}s} \exp(i\mathbf{k}\cdot\mathbf{r}) - \text{c.c}\}. \tag{2.37}$$

2.2.1 Quantization procedure

In order for us to quantize the field, it is necessary that we associate the Hilbert space operators with the dynamical variables, which in principle do not commute. In the Hilbert space, the classical variables $q_{\mathbf{k}s}(t)$ and $p_{\mathbf{k}s}(t)$ are denoted by $\hat{q}_{\mathbf{k}s}(t)$ and $\hat{p}_{\mathbf{k}s}(t)$ respectively. As it is stated in the postulate of quantum mechanics, each pair of these canonical conjugate operators $\hat{q}_{\mathbf{k}s}(t)$ and $\hat{p}_{\mathbf{k}s}(t)$ satisfies a non-zero commutator $i\hbar$. While the classical variables associated with the two different modes are understood to be uncoupled, the corresponding Hilbert space operators commute. The set of commutation relations reads as

$$[\hat{q}_{\mathbf{k}s}(t), \hat{p}_{\mathbf{k}'s'}(t)] = i\hbar \delta^3_{\mathbf{k}\mathbf{k}'} \delta_{ss'}, \tag{2.38}$$

$$[\hat{q}_{\mathbf{k}s}(t), \hat{q}_{\mathbf{k}'s'}(t)] = 0, \tag{2.39}$$

$$[\hat{p}_{\mathbf{k}s}(t), \hat{p}_{\mathbf{k}'s'}(t)] = 0. \tag{2.40}$$

The dynamical variables are to be considered as Hilbert space operators which happen not to commute. Furthermore, all the above expressions of the expansions such as Eqs. (2.20), (2.23), (2.24) together with the equations of motions in Eqs. (2.16), (2.30), (2.31) remain valid operator equations. Hence, the Hamiltonian of the quantized radiation field becomes

$$\hat{H} = \frac{1}{2} \sum_{\mathbf{k}} \sum_{s=1}^{2} [\hat{p}^2_{\mathbf{k}s}(t) + \omega^2_{\mathbf{k}s} \hat{q}^2_{\mathbf{k}s}(t)]. \tag{2.41}$$

It is well understood that these operators $\hat{q}_{\mathbf{k}s}(t)$ and $\hat{p}_{\mathbf{k}s}(t)$ together with the field vectors $\hat{\mathbf{A}}(\mathbf{r},t)$, $\hat{\mathbf{E}}(\mathbf{r},t)$, $\hat{\mathbf{B}}(\mathbf{r},t)$, etc., are dynamical variables, whereas the space-time variables $\mathbf{r}$, t only participate in the role of being parameters. For many reasons it is advisable not to deal with the real dynamical variables or the Hermitian operators but to chose to work with a set of non-Hermitian operators of the form

$$\hat{a}_{\mathbf{k}s}(t) = \frac{1}{\sqrt{2\hbar\omega_{\mathbf{k}s}}}[\omega_{\mathbf{k}s}\hat{q}_{\mathbf{k}s}(t) + i\hat{p}_{\mathbf{k}s}(t)], \tag{2.42}$$

$$\hat{a}^{\dagger}_{\mathbf{k}s}(t) = \frac{1}{\sqrt{2\hbar\omega_{\mathbf{k}s}}}[\omega_{\mathbf{k}s}\hat{q}_{\mathbf{k}s}(t) - i\hat{p}_{\mathbf{k}s}(t)]. \tag{2.43}$$

The expression in Eq. (2.43) is the Hermitian conjugate of Eq. (2.42). We can also invert these equations such that all the operators $\hat{q}_{\mathbf{k}s}(t)$ and $\hat{p}_{\mathbf{k}s}(t)$ can be expressed in terms of $\hat{a}_{\mathbf{k}s}(t)$ and $\hat{a}^{\dagger}_{\mathbf{k}s}(t)$ operators:

$$\hat{q}_{\mathbf{k}s}(t) = \sqrt{\frac{\hbar}{2\omega_{\mathbf{k}s}}}[\hat{a}_{\mathbf{k}s}(t) + \hat{a}^{\dagger}_{\mathbf{k}s}(t)], \tag{2.44}$$

$$\hat{p}_{\mathbf{k}s}(t) = i\sqrt{\frac{\hbar\omega_{\mathbf{k}s}}{2}}[\hat{a}_{\mathbf{k}s}(t) - \hat{a}^{\dagger}_{\mathbf{k}s}(t)]. \tag{2.45}$$

With the help of Eqs. (2.38) to (2.40), we can easily determine the corresponding commutation relations for the $\hat{a}_{\mathbf{k}s}(t)$ and $\hat{a}^{\dagger}_{\mathbf{k}s}(t)$ to be

$$[\hat{a}_{\mathbf{k}s}(t), \hat{a}^{\dagger}_{\mathbf{k}'s'}(t)] = \delta^{3}_{\mathbf{k}\mathbf{k}'}\delta_{ss'}, \tag{2.46}$$

$$[\hat{a}_{\mathbf{k}s}(t), \hat{a}_{\mathbf{k}'s'}(t)] = 0, \tag{2.47}$$

$$[\hat{a}^{\dagger}_{\mathbf{k}s}(t), \hat{a}^{\dagger}_{\mathbf{k}'s'}(t)] = 0. \tag{2.48}$$

Let us consider the rescaled operators of the momentum and position such that the operators $\hat{a}_{\mathbf{k}s}(t)$ and $\hat{a}^{\dagger}_{\mathbf{k}s}(t)$ correspond to the complex amplitudes $u_{\mathbf{k}s}(t)$ and $u^{*}_{\mathbf{k}s}(t)$. They have the same time dependence as in Eq. (2.21),

$$\hat{a}_{\mathbf{k}s}(t) = \hat{a}_{\mathbf{k}s}(0)\exp(-i\omega_{\mathbf{k}s}t), \tag{2.49}$$

$$\hat{a}^{\dagger}_{\mathbf{k}s}(t) = \hat{a}_{\mathbf{k}s}(0)\exp(i\omega_{\mathbf{k}s}t). \tag{2.50}$$

The product of these operators $\hat{a}_{\mathbf{k}s}(t)\hat{a}^{\dagger}_{\mathbf{k}s}(t)$ and $\hat{a}^{\dagger}_{\mathbf{k}s}(t)\hat{a}_{\mathbf{k}s}(t)$ are thus time dependent. However, if we substitute $\hat{q}_{\mathbf{k}s}(t)$ and $\hat{p}_{\mathbf{k}s}(t)$ given in Eqs. (2.44) and (2.45) into the Hamiltonian form Eq. (2.41) we get

$$\hat{H} = \frac{1}{2}\sum_{\mathbf{k}}\sum_{s=1}^{2}\hbar\omega_{\mathbf{k}s}[\hat{a}_{\mathbf{k}s}(t)\hat{a}^{\dagger}_{\mathbf{k}s}(t) + \hat{a}^{\dagger}_{\mathbf{k}s}(t)\hat{a}_{\mathbf{k}s}(t)]. \tag{2.51}$$

If we use the commutation relation in Eq. (2.46), we can find an alternative way to express $\hat{H}$ in the normally ordered form to be

$$\hat{H} = \sum_{\mathbf{k}}\sum_{s=1}^{2}\hbar\omega_{\mathbf{k}s}[\hat{a}^{\dagger}_{\mathbf{k}s}(t)\hat{a}_{\mathbf{k}s}(t) + \frac{1}{2}], \tag{2.52}$$

where $\hat{a}^{\dagger}_{\mathbf{k}s}(t)$ and $\hat{a}_{\mathbf{k}s}(t)$ represent the creation and annihilation operators, respectively. The term $\frac{1}{2}\hbar\omega_{\mathbf{k}s}$ contributes to the energy of each $\mathbf{k}$, whereas s the oscillator mode is the zero point contribution. If we chose to omit the zero point energy contribution we can always chose the vacuum energy to be zero, since it does not affect the particular dynamics and the global phase in Eq. (2.52), then the corresponding Hamiltonian becomes

$$\hat{H}(t) = \sum_{\mathbf{k}}\sum_{s=1}^{2}\hbar\omega_{\mathbf{k}s}\hat{a}^{\dagger}_{\mathbf{k}s}(t)\hat{a}_{\mathbf{k}s}(t). \tag{2.53}$$

Furthermore, we can re-write the expansions for the field operators in Eqs. (2.35)-(2.37) as follows

$$\hat{\mathbf{A}}(\mathbf{r},t) = \frac{1}{L^{3/2}}\sum_{\mathbf{k},s}\Big(\frac{\hbar}{2\varepsilon_0\omega_{\mathbf{k}s}}\Big)^{1/2}[\hat{a}_{\mathbf{k}s}(0)\varepsilon_{\mathbf{k}s}\exp[i(\mathbf{k}\cdot\mathbf{r} - \omega_{\mathbf{k}s}t)] + \text{h.c}], \tag{2.54}$$

$$\hat{\mathbf{E}}(\mathbf{r},t) = \frac{1}{L^{3/2}}\sum_{\mathbf{k},s}\Big(\frac{\hbar\omega_{\mathbf{k}s}}{2\varepsilon_0}\Big)^{1/2}[i\hat{a}_{\mathbf{k}s}(0)\varepsilon_{\mathbf{k}s}\exp[i(\mathbf{k}\cdot\mathbf{r} - \omega_{\mathbf{k}s}t)] + \text{h.c}], \tag{2.55}$$

$$\hat{\mathbf{B}}(\mathbf{r},t) = \frac{1}{L^{3/2}}\sum_{\mathbf{k},s}\Big(\frac{\hbar}{2\varepsilon_0\omega_{\mathbf{k}s}}\Big)^{1/2}[i\hat{a}_{\mathbf{k}s}(0)(\mathbf{k}\times\varepsilon_{\mathbf{k}s})\exp[i(\mathbf{k}\cdot\mathbf{r} - \omega_{\mathbf{k}s}t)] + \text{h.c}], \tag{2.56}$$

where h.c represents the Hermitian conjugate.

Chapter 3

Adoptation of the generic Hamiltonians for the needs of numerical simulations

In this chapter, we present a brief discussion on the model that was adopted to conduct the numerical simulations. In addition to that, we further present the Hamiltonian of the whole system. Afterward, we will look into the details of how the whole numerical simulations of quantum electrodynamics were generated since that is understood to be the core of this thesis.

3.1 Two-level atom approximation

The quantum treatment of light interacting with atoms was vital in the progressive development of quantum theory in the mid-twentieth century. However, real atoms are quite complex systems. Even the hydrogen atom which is seen as the simplest atom has a non-trivial energy level structure. As a result, it is necessary for one to approximate the behaviour of a atom by making use of a much simpler quantum system. The two level atom approximation was developed to interpret the interaction between light and atoms. For such reasons, it is understood that only two sets of atomic energy levels E_1 and E_2 are applicable in the interaction with the quantized electromagnetic field. In principle, an atom is believed to have many quantum levels of different energy and within these levels there are many possibilities of optical transitions. However, in the two-level approximation only the specific transition that satisfies Eq. (2.1) is

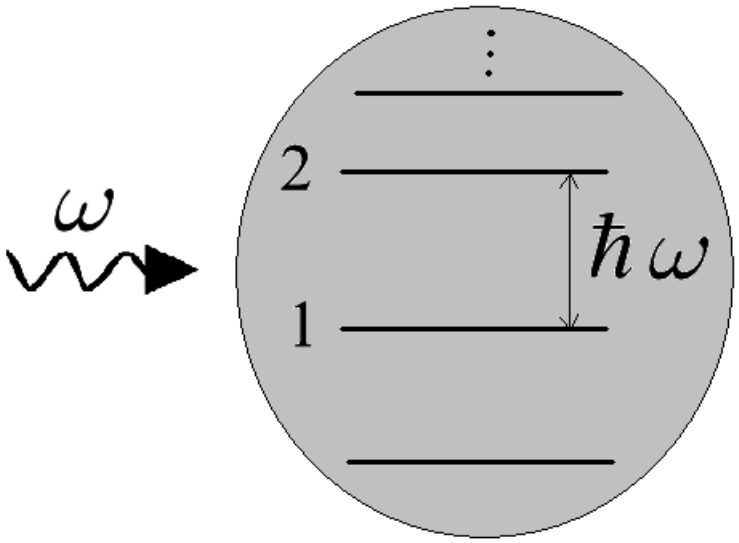

Figure 3.1: The two-level atom approximation.

considered and the rest of the levels are neglected. Therefore, it is necessary to label the lower and upper levels as 1 and 2 respectively as shown in Fig. 3.1.

The physical basis for the two-level approximation is designed to accommodate the process of resonance. Nonetheless in the classical picture of light interacting with an atom, it is indicated that the light beam stimulates the dipole oscillations in the atom, and consequently the light re-radiates at the same frequency. If the frequency of the light is in line to the natural frequency of the resonant atom, then the magnitude of the dipole oscillations will be large and the light-atom interaction will be strong. Similarly, if the frequency of light is a distant apart from the natural frequency of the atom (off-resonance), then the magnitude of controlled oscillations will be small, so as the interaction between the light and the atom. In other words, the light-atom interaction is said to be quite strong in the resonant case as compared to the off-resonant transitions. In the next section we present the Hamiltonian of the system.

3.2 The Hamiltonian of the system

In the previous section expressions for the full Hamiltonian of the free electromagnetic field were derived. In this section the total Hamiltonian of the system describing the interaction between the two-level atoms and quantized field is presented as the sum of the field, atomic and interaction Hamiltonian of the form

$$\hat{H} = \hat{H}_F + \hat{H}_A + \hat{H}_I, \tag{3.1}$$

where $\hat{H}_F$ is the field Hamiltonian given by the expression in Eq. (2.53) whereas the atomic and the interaction Hamiltonian, $\hat{H}_A$ and $\hat{H}_I$ respectively, shall be derived in the sections that follow.

3.2.1 The Hamiltonian of a two-level system

In addition to the field, in this section the Hamiltonian of the two-level system is presented. The assumption is that, the two level system has an energy, which consists of a ground state, denoted by $|g\rangle$ with energy E_g and an excited state denoted by $|e\rangle$, with energy $E_e = \hbar\omega_0 + E_g$. The two-dimensional states are represented as vectors in $\mathbb{C}^2$. The Hamiltonian operator of the two level atoms in the energy representation is given as [18]

$$\hat{H}_A = E_e \left|e\right\rangle \left\langle e\right| + E_g \left|g\right\rangle \left\langle g\right|. \tag{3.2}$$

This Hamiltonian can be transformed to a more convenient form, if one chooses to define the level of the energy to be zero halfway between the state $|e\rangle$ and $|g\rangle$ as shown in Fig. 3.2. If we introduce the Pauli spin operator to be $\hat{\sigma}_z = |e\rangle\langle e| - |g\rangle\langle g|$ and take into account the identity representation $\mathbb{1} = |e\rangle\langle e| + |g\rangle\langle g|$ in $\mathbb{C}^2$, it is straightforward to see that, the free atomic Hamiltonian in Eq. (3.2) may be written as

$$\hat{H}_A = E_e\left(\frac{\mathbb{1}}{2} + \frac{\sigma_z}{2}\right) + E_g\left(\frac{\mathbb{1}}{2} - \frac{\sigma_z}{2}\right), \tag{3.3}$$

$$= (E_e - E_g)\frac{\sigma_z}{2} + (E_e + E_g)\frac{\mathbb{1}}{2}, \tag{3.4}$$

$$= \frac{\hbar\omega_0}{2}\sigma_z + \left(\frac{E_e + E_g}{2}\right)\mathbb{1}. \tag{3.5}$$

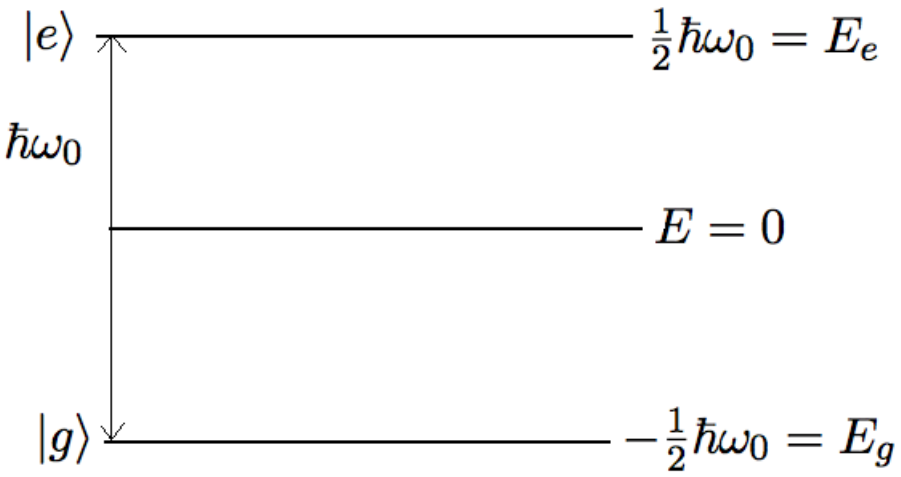

Figure 3.2: An atom energy level diagram, with E=0 level at the middle between the states $|g\rangle$ and $|e\rangle$, respectively.

where $(E_e - E_g) = \hbar\omega_0$, respectively. We drop the term which is proportional to the identity since it does not contribute to the dynamics and only contribute to the global phase. Then, the Hamiltonian that describes a set of N_A, non-interacting two-level atoms becomes

$$\hat{H}_A = \frac{1}{2}\sum_{j=1}^{N_A} \hbar\omega_j \hat{\sigma}_z^j. \tag{3.6}$$

where ω_j denotes the transition frequency of the jth atom.

3.2.2 The interaction Hamiltonian between light and matter in quantum optics

In the previous sections, the quantum-mechanical description of the energy contributions of the field and the two-level system were derived. In this section, we introduce

the energy contribution that arises from the interaction of the quantized electromagnetic field and the two-level system. Assuming that the wavelength of the field is much larger than the dimension of the atom, then the atom-field interaction will emerge by treating the atom as an electric dipole. In quantum optics, the dipole approximation is understood to be correct. In the general case, in the quantum theory the atom-field interaction Hamiltonian can be described by the quantized electric-dipole approximation of the form [1, 2, 19]

$$\hat{H}_{\text{Int}} = -\hat{\mathbf{d}} \cdot \hat{\mathbf{E}}(\vec{\mathbf{R}}, t), \tag{3.7}$$

where the vector $\vec{\mathbf{R}}$ denotes the position of the atom. In particular, the term $\hat{\mathbf{d}}$ is the dipole moment and can be expressed by

$$\hat{\mathbf{d}} = \mathbf{d}_{ge}\hat{\sigma}_- + \mathbf{d}_{eg}\hat{\sigma}_+, \tag{3.8}$$

where $\hat{\sigma}_- = |g\rangle\langle e|$ and $\hat{\sigma}_+ = |e\rangle\langle g|$. However, here we applied the property that the states $|g\rangle$ and $|e\rangle$ have opposite parity such that $\langle g|\,\hat{\mathbf{r}}\,|g\rangle = \langle e|\,\hat{\mathbf{r}}\,|e\rangle = 0$, respectively. The term $\hat{\mathbf{E}}(\vec{\mathbf{R}}, t)$ in Eq. (3.7) represents the electric field given in Eq. (2.55). If we substitute Eq. (2.55) and Eq. (3.8) into Eq. (3.7) we get the interaction Hamiltonian of the form

$$\hat{H}_{\text{Int}} = -\left(\mathbf{d}_{ge}\hat{\sigma}_- + \mathbf{d}_{eg}\hat{\sigma}_+\right) \cdot \sqrt{\frac{\hbar\omega}{2\varepsilon_0}}[\mathbf{u}(\mathbf{R})\hat{a} + h.c], \tag{3.9}$$

$$= -\hbar g(\hat{\sigma}_- + \hat{\sigma}_+)(\hat{a} + \hat{a}^\dagger), \tag{3.10}$$

where $\mathbf{u}(\mathbf{R})$ is the mode function of the field given by $\mathbf{u}(\mathbf{R}) = \frac{1}{L^{3/2}}\varepsilon_{ks}\exp(i\mathbf{k}\cdot\mathbf{R})$, and we assume that $\hbar g = \mathbf{d}_{ge} \cdot \mathbf{u}(\mathbf{R})\sqrt{\hbar\omega/(2\varepsilon_0)}$. However, we can re-write the interaction Hamiltonian in Eq. (3.10) as

$$\hat{H}_{\text{Int}} = -\hbar g(\hat{\sigma}_+\hat{a} + \hat{\sigma}_-\hat{a}^\dagger + \hat{\sigma}_-\hat{a} + \hat{\sigma}_+\hat{a}^\dagger), \tag{3.11}$$

$$= -\hbar g(\hat{\sigma}_+\hat{a} + \hat{\sigma}_-\hat{a}^\dagger), \tag{3.12}$$

For simplicity, we have invoked the rotating wave approximation in Eq. (3.11). The last two terms were neglected because they violate the conservation of number of

excitations [20]. Furthermore, in 2-D we have the transversality condition and of course there are two-polarisations, but we can chose them in such a way that one polarisation is always outside of the 2-D. If that is the case, we end up with a wave vector and one polarisation. If we look into a case of 1-D there are no polarisation at all since there is no k-vector which, implies that there is no directions. Finally, if we drop the index s from Eq. (2.53), and insert it together with Eq. (3.6) and Eq. (3.12) into the total Hamiltonian Eq. (3.1) we get the new Hamiltonian in the rotating wave approximation (RWA) [21]

$$\hat{H} = \sum_k \hbar\omega_k \hat{a}_k^\dagger \hat{a}_k + \frac{1}{2}\sum_{j=1}^{N_A} \hbar\omega_j \hat{\sigma}_z^j + \sum_k \sum_{j=1}^{N_A} \hbar(g\hat{a}_k \hat{\sigma}_+^j + g^* \hat{a}_k^\dagger \hat{\sigma}_-^j). \tag{3.13}$$

Essentially, Eq. (3.13) describes the whole quantum-mechanical system of two-level atoms interacting with discrete field modes. In the next sections, we give an outline on how the numerical simulations of quantum electrodynamics were conducted together with the numerical scheme.

3.3 Details of the model and the calculations

We begin our investigation of light-matter interaction by considering some basic ideas from the classical regime of radiation. We want to re-produce a simulation of QED in the quantum optical regime. The idea here is to exactly demonstrate what the authors of [13] have done which is all classical optics but at the quantum mechanical level.
The quantum mechanical treatment of the interaction between the light and quantum mirrors is based on how the mirror is simulated. A mirror is a material that is made up of a collection of atoms and the light it interacts with doesn't only get reflected but it is being absorbed and re-emitted by these atoms. Similarly, if we took some atoms off-resonance we get an interference pattern which allows us to simulate a beam-splitter. We take into account all these statements from the classical optics point of view and apply them directly to quantum mechanics. The motivation for our work, is to demonstrate these QED simulations [13].

We are going to begin the simulations by first working out the energy densities of the single photon in different two-dimensional atomic arrangements. We are going to

adopt the model put forward in [13] to indicate how the calculations were conducted together with the simulations. As in the 3-D case, we can show that the quantization in 2-D allows us to introduce the energy-density operator that is contained in both the electric and magnetic fields as:

$$\hat{\mathbf{H}} = \frac{1}{2}\epsilon_0 \hat{\mathbf{E}}^2 + \frac{1}{2\mu_0}\hat{\mathbf{B}}^2, \tag{3.14}$$

and μ_0 is the magnetic constant permeability of free space vacuum permeability, whereas $\hat{\mathbf{E}}$, $\hat{\mathbf{B}}$ denotes the electric and magnetic field. We will then make use of these results to describe the interaction of the photon with a collection of two-level atoms inside the two-dimensional cavity. Using the expansions of the electric and magnetic fields [17], these two terms in Eq. (3.14) become

$$\frac{1}{2}\epsilon_0 \hat{\mathbf{E}}^2 = \frac{\hbar}{2L^2} R R^*, \tag{3.15}$$

$$\frac{1}{2\mu_0}\hat{\mathbf{B}}^2 = \frac{\hbar}{2L^2\epsilon_0\mu_0}(S_x S_x^* + S_y S_y^*), \tag{3.16}$$

where R and S_i are the Fourier transforms of the two different functions;

$$R = \sum_k \sqrt{\omega_k} c_k \exp(i\mathbf{k}\cdot\mathbf{r}), \tag{3.17}$$

$$S_i = \sum_i \frac{k_i}{\sqrt{\omega_k}} c_k \exp(i\mathbf{k}\cdot\mathbf{r}), \qquad i = x, y. \tag{3.18}$$

We take into account that the polarisation is one. Substituting all these expressions Eq. (3.15)-(3.18) into Eq. (3.14) yields

$$\hat{\mathbf{H}} = \frac{c\hbar}{2L^2}\sum_{k,k'} c_k c_{k'}^* \exp[i(\mathbf{k}-\mathbf{k}')\cdot\mathbf{r}]\left[\sqrt{|\ k|\cdot|\ k'|} + \frac{k_x k_x' + k_y k_y'}{\sqrt{|\ k|\cdot|\ k'|}}\right]. \tag{3.19}$$

In general, if we know the value of the coefficient c_k in Eq. (3.19) we can calculate the energy density of the field inside an empty two-dimensional cavity. The choice of the general state vector in all our simulations has the following form

$$|\Psi\rangle = \sum_k c_k |1_k, 0\rangle + \sum_{j=1}^{N_A} c_j |0, 1_j\rangle, \tag{3.20}$$

where N_A is the total number of atoms. The basis functions $|0\rangle_j$ and $|1\rangle_j$ are the two-internal states of the j^{th} atom and the general Gaussian of one-photon state vector is of the following form

$$|\Psi\rangle = \sum_k c_k \, |1_k, 0\rangle \, , \tag{3.21}$$

where the mode coefficient c_k is given as

$$c_k = (2\pi\Delta_{kx}^2)^{-1/4}(2\pi\Delta_{ky}^2)^{-1/4} \exp(-i\mathbf{k}\cdot\mathbf{r_0}) \exp\Big\{ -\frac{(k_x - k_{x0})^2}{4\Delta_{kx}^2} - \frac{(k_y - k_{y0})^2}{4\Delta_{ky}^2} \Big\}. \tag{3.22}$$

The mode coefficient c_k in Eq. (3.22) represents the initial distribution used in all our simulations. In order to proceed, we then need to work out the interaction Hamiltonian in the RWA and the state vector associated to it. This will allow us to determine the Schrödinger equation which will be used extensively in the next part of the numerical methods. Essentially the Schrödinger equation has the form

$$i\hbar|\dot{\Psi}\rangle = H|\Psi\rangle \tag{3.23}$$

where H is given by

$$H = H_0 + H_I, \tag{3.24}$$

where the H_0 is the free Hamiltonian and H_I is the interaction Hamiltonian. In the paper [13], the authors reverts to the interaction picture with respect to H_0, however here we choose to stay in the Schrödinger picture. The free Hamiltonian H_0 reads as;

$$H_0 = \sum_k \hbar\omega_k a_k^\dagger a_k + \sum_j \hbar\frac{\omega_j}{2}\sigma_z^j, \tag{3.25}$$

and the interaction Hamiltonian H_{I} in the RWA approximation has the form

$$H_{\mathrm{I}} = \sum_j \sum_k g_{jk}\sigma_+^j a_k + g_{jk}^*\sigma_-^j a_k^\dagger. \tag{3.26}$$

The total Hamiltonian H commutes with the number of excitations operator

$$\hat{N} = \sum_k a_k^\dagger a_k + \sum_j \sigma_z^j, \tag{3.27}$$

such that $[\hat{H}, \hat{N}] = 0$. This implies that if initially there is only one photon in the field and no excitation in the atoms then the total number of excitations is one and it is conserved. The general state vector in Eq. (3.20) becomes

$$|\Psi\rangle = \sum_k c_k(t) \, |1_k\rangle + \sum_j c_j(t) \, |1_j\rangle \, . \tag{3.28}$$

The first term represents the excitation in one of the modes of the field, and the second term represents the excitation in one the atoms. The state vector $|\dot{\Psi}\rangle$ is as follows;

$$|\dot{\Psi}\rangle = \sum_k \dot{c}_k(t) \, |1_k\rangle + \sum_j \dot{c}_j(t) \, |1_j\rangle \, . \tag{3.29}$$

Let us first determine what happens when H_0 acts on the state vector in Eq. (3.28). Mathematically, we get that

$$H_0 \, |\Psi\rangle = \sum_k \sum_{k'} (\hbar \omega_{k'} a_{k'}^\dagger a_{k'}) c_k \, |1_k\rangle + \sum_j \sum_{j'} (\hbar \frac{\omega_{j'}}{2} \sigma_z^{j'}) c_j \, |1_j\rangle \, . \tag{3.30}$$

In the first term only the k-components acts on the k-state. The same applies to the second term. Furthermore, when the k-components acts on $|1_j\rangle$ we get zero, so as for the j-components on $|1_k\rangle$, respectively. In addition, we note that k' is the number of photons in the mode, so we can only have 1-photon on the $k-th$ mode and the rest becomes zero. So when k acts on k' the result won't be zero provided $k = k'$ and the same thing applies for the $j-th$ atom case. So the end result becomes

$$H_0 \, |\Psi\rangle = \sum_k \hbar \omega_k c_k \, |1_k\rangle + \sum_j \frac{\hbar \omega_j}{2} c_j \, |1_j\rangle \, . \tag{3.31}$$

We will now work out the next step, that is H_{I} acting on the state vector in Eq. (3.28) as follows

$$H_I\,|\Psi\rangle = \Big[\sum_{j'}\sum_{k'} g_{j'k'}\sigma_+^{j'}a_{k'} + g^*_{j'k'}\sigma_-^{j'}a^\dagger_{k'}\Big]\Big(\sum_k c_k\,|1_k\rangle + \sum_j c_j\,|1_j\rangle\Big), \tag{3.32}$$

$$= \sum_k\sum_{j'} g_{j'k}c_k\,|1_j\rangle + \sum_j\sum_{k'} g^*_{jk'}c_j\,|1_{k'}\rangle\,. \tag{3.33}$$

If we neglect the primes, since it's just indices we get

$$H_I\,|\Psi\rangle = \sum_k\sum_{j'} g_{j'k}c_k\,|1_j\rangle + \sum_j\sum_{k'} g^*_{jk'}c_j\,|1_{k'}\rangle\,. \tag{3.34}$$

If we re-write Eq. (3.23) as

$$|\dot{\Psi}\rangle = -\frac{i}{\hbar}H|\Psi\rangle, \tag{3.35}$$

and substitute Eq. (3.31) and Eq. (3.34) into Eq. (3.35) we get

$$-\frac{i}{\hbar}H|\Psi\rangle = \sum_k \dot{c}_k\,|1_k\rangle + \sum_j \dot{c}_j\,|1_j\rangle = |\dot{\Psi}\rangle. \tag{3.36}$$

By equating terms with the same basis vectors $|1_k\rangle$ and $|1_j\rangle$ in Eq. (3.36) one can rewrite the Schrödinger equation in Eq. (3.36) as system of linear differential equations with constant coefficient for the components of the total wave function $|\Psi\rangle$ as follows;

$$\begin{aligned}\dot{c}_k &= -\,i\omega_k c_k - \frac{i}{\hbar}\sum_j g^*_{jk}c_j,\\ \dot{c}_j &= -\frac{i\omega_j}{2}c_j - \frac{i}{\hbar}\sum_j g_{jk}c_k,\end{aligned} \tag{3.37}$$

where the term g_{jk} is the coupling constant given by

$$g_{jk} = -\frac{i\hbar}{2\varepsilon_0 L}\sqrt{\omega_k}D_j\exp(i\mathbf{k}\cdot\mathbf{r}_j). \tag{3.38}$$

We can approximate the frequency of the field ω_k by the frequency of the atoms ω_j since we assume that the interaction is happening in close resonance, then g_{jk} becomes

$$g_{jk} \approx -\frac{i\hbar}{2\varepsilon_0 L}\sqrt{\omega_j} D_j \exp(i\mathbf{k}\cdot\mathbf{r}_j). \tag{3.39}$$

We can efficiently solve the system of linear equations in Eq. (3.37) provided we re-write it in the form of Fourier transform algorithm since we chose to work with the number of modes to be of the power of two i.e; 256 and 1024 modes which allows us to implement the fast Fourier transform (FFT). If we substitute the term g_{jk} into Eq. (3.37), the sets of linear equations can be written in the form of the Fourier transform algorithm

$$\begin{aligned} \dot{c}_k =& -i\omega_k c_k + \sum_{\mathbf{r}} \left(\sum_j \frac{\sqrt{\omega_j} D_j^*}{2\varepsilon_0 L} c_j \delta(\mathbf{r}-\mathbf{r}_j) \right) \exp(-i\mathbf{k}\cdot\mathbf{r}), \\ \dot{c}_j =& -\frac{i\omega_j}{2} c_j - \frac{\sqrt{\omega_j} D_j}{2\varepsilon_0 L} \sum_k c_k \exp(i\mathbf{k}\cdot\mathbf{r}). \end{aligned} \tag{3.40}$$

For our simulations, it is necessary that we work directly with the $\dot{c}_k$ and $\dot{c}_j$ in Eq. (3.40) as functions of the two-dimensional Fourier transforms. In essence, the wave function $|\dot{\Psi}\rangle$ is a set of these two matrices $(\dot{c}_k)$ and $(\dot{c}_j)$. The mirror and beam splitter are materials constructed from a group of atoms arranged into an elongated atomic slab inside the cavity. We created some spacing mirrors and beam splitters as a matrix with one's off-diagonal right at the centre and zeroes elsewhere. Furthermore, in order to apply the Runge-Kutta of the 4th order (RK4) as our choice of mathematical tool, we had to define the function $\hat{H}(t_n)$ which will take in two arguments that is (c_k, c_j) at any moment of time (t) and give out two new matrices. In the next section we illustrate how we worked out the numerical results. In principle, the expression in Eq. (3.35) is a differential equation. Since all our numerical simulations were done in the Schrödinger picture, we will solve numerically this time dependent Schrödinger problem in order to propagate the Gaussian wave packet coupled to a group of atoms.

3.4 Numerical methods in 1-D and 2-D

In this section, we provide an overview on how the numerical simulations were conducted. We begin by indicating a mathematical tool that was applied to integrate the

time dependent Schrödinger equation in Eq. (3.35). In addition, for our expression we are solving numerically the right hand side of this differential equation. In our simulations, this operation of $\hat{H}\,|\Psi(t)\rangle$ is used quite often. We utilize the classical fourth order Runge-Kutta method to work out this integration of the time dependent Schrödinger's equation. Suppose a wavefunction at time t_n is given by $|\Psi(t_n)\rangle$ then at a later time (t_{n+1}) the wavefunction will be given by the following algorithm [22]

$$|k_1\rangle = -\frac{i}{\hbar}\hat{H}\Big(t_n\Big)\,|\Psi(t_n)\rangle\,, \tag{3.41}$$

$$|k_2\rangle = -\frac{i}{\hbar}\hat{H}\Big(t_n+\frac{h}{2}\Big)\Big(\,|\Psi(t_n)\rangle+\frac{h}{2}\,|k1\rangle\,\Big), \tag{3.42}$$

$$|k_3\rangle = -\frac{i}{\hbar}\hat{H}\Big(t_n+\frac{h}{2}\Big)\Big(\,|\Psi(t_n)\rangle+\frac{h}{2}\,|k2\rangle\,\Big), \tag{3.43}$$

$$|k_4\rangle = -\frac{i}{\hbar}\hat{H}\Big(t_n+h\Big)\Big(\,|\Psi(t_n)\rangle+h\,|k3\rangle\,\Big), \tag{3.44}$$

$$|\Psi(t_{n+1})\rangle = |\Psi(t_n)\rangle + h\Big(\frac{|k1\rangle}{6}+\frac{|k2\rangle}{3}+\frac{|k3\rangle}{3}+\frac{|k4\rangle}{6}\Big)+O((\triangle t)^5), \tag{3.45}$$

where the index n and $n+1$ are time discretization and h is the step in time size; they are determined by total time (T) to run the simulation per number of steps (n). Essentially, this form of integration works quite well to determine the right hand side of Eq. (3.35) respectively. In principle the authors of the paper [13] have done the simulations in the interaction picture, however in this work we have done the simulations in the Schrödinger picture.

3.5 Simulation Scheme in 1-D and 2-D

Here we present a scheme on how the numerical results were conducted. In our work all the numerical simulations were done in Mathematica. The initial state of the field in these simulations is a general Gaussian Eq. (3.22). First we defined k as the two-dimensional array for all possible values of k in the (x, y) space, by creating a table function for it. We consider c_k in Eq. (3.22) as the coefficient of the photonic wave function. We calculate the sequence of the c_k's for some time interval to generate the time evolution of the field. For the free-evolution it is necessary that we work directly with the c_k to determine the energy densities of the field and how they behave. Start-

ing with the c_k, we then apply the Fourier transform to generate the matrices of the formulas for R and S_i in Eq. (3.17) and Eq. (3.18). Afterwards, we put everything together into Eq. (3.19) and form the matrices for the Hamiltonian for every field. Finally, we plotted diagrams for the energy densities to propagate the photon wave packet for the time evolution in free-space, respectively.

The mirror and beam splitter simulations were both done in 1-D and 2-D. Both the mirrors and the beam splitters were created from a spacing matrix which consists of a number of atoms inlined to seven layers of atoms where there is a mirror and one layer of atoms where there is beam splitter. We then calculated a sequence of the c_k's from Eq. (3.22) in order for us to work the Fourier transform from Eq. (3.17) and Eq. (3.18).

For simulations in 1-D we calculated the matrices for every Hamiltonian of the field for only the x-components. Afterwards we simulated Eq. (3.40) by utilising the mathematical tool Fourier and inverse Fourier transform and Runge-Kutta method. It is only necessary that we simulate the sets of linear equations in order to demonstrate how the wave function propagate from time (t_n) to (t_{n+1}), respectively. We propagate the wave function by dividing the time we want to simulate for a number of steps which gives us discretization in time. Also, in 2-D simulations we applied the same procedure except that the matrices for the Hamiltonian of the field were determined in both x and y-components. In the next section, we present the results of numerical simulations we were able to produce.

Chapter 4

Results and Discussion

Now we want to present the numerical results. We simulated the time dependent Schrödinger equation in Eq. (3.35). In the previous chapter, it is demonstrated how we performed the calculations in order to conduct the simulations. Afterwards, it was shown how we generated the time evolution of the energy densities for a finite number of steps. Furthermore, we have demonstrated how a group of atoms were used to build mirror and beam splitter for the radiation.
We present the simulations as follows, we begin our simulations by demonstrating the behaviour of a free photon inside an empty cavity. In the next section 4.2, we add a group of atoms inside the cavity and perform simulations of a photon interacting with the atoms of the (mirrors and beam splitters). In these sections, we have carried out the simulations in both 1-D and 2-D system. In each and every simulation we have included the time dependence on the numerical calculations of $|\psi|^2$ plots. These plots of the trace demonstrates the consistency of norm of the total wave-function during numerical simulation.

4.1 A free photon simulation

In the first simulation, we show the time evolution of a free photon. There are no atoms inside the cavity, only the field is present. The initial wave packet is given by the Gaussian in Eq. (3.22). The time evolution of the energy density distribution at various time steps is shown in Figure (4.1). The photon wave packet propagates to the right as the number of time steps increases. The energy density becomes delocalized during the free evolution. Later on the width of the wave packet spread out along

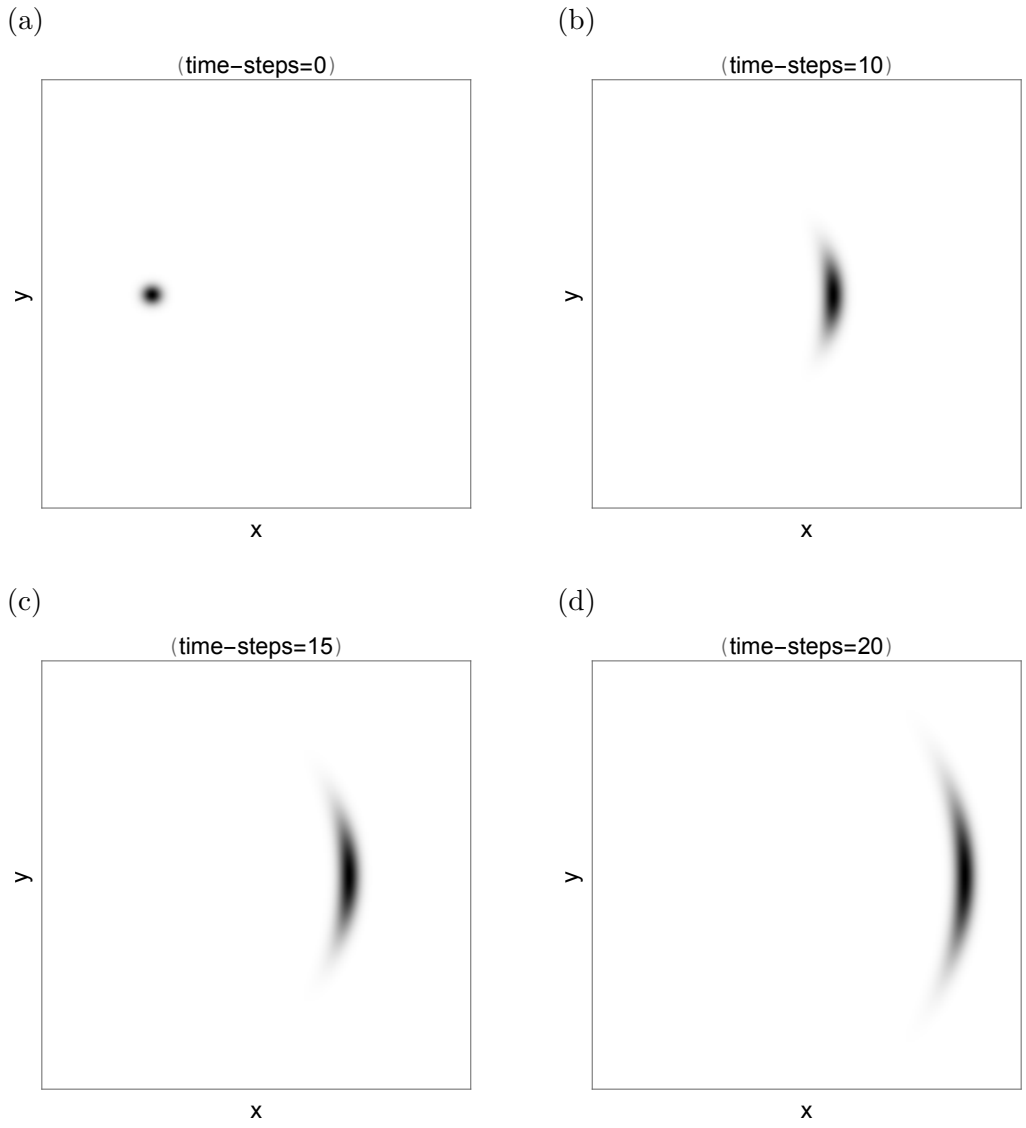

Figure 4.1: The sequence of time evolutions of the energy density of a free-photon in Eq. (3.19) with the initial Gaussian wave packet in Eq. (3.22) inside an empty cavity. The parameters are x0=-8.0, y0=0.0, $k_{x0} = 5.0$, $k_{y0} = 0$, $\triangle_{kx}^2$=$\triangle_{ky}^2$=1.0, $\omega_j = 5.0$, $D_j = 0.5$ and the number of modes (N=256) with the size of the cavity L=10π. In Fig. 4.1(a), the wave packet is well localized while in Fig. 4.1(d) it has changed its initial shape, with the wave packet spreading along the y-direction.

the y-direction. This spread of the width occurs because of the standard quantum-mechanical effect, since the mode-spectrum of the wave packet in the **k**-space happens to be relatively broad and close to the origin. In the next sections, we add an ensemble of atoms and carry the simulations in 1-D and in 2-D.

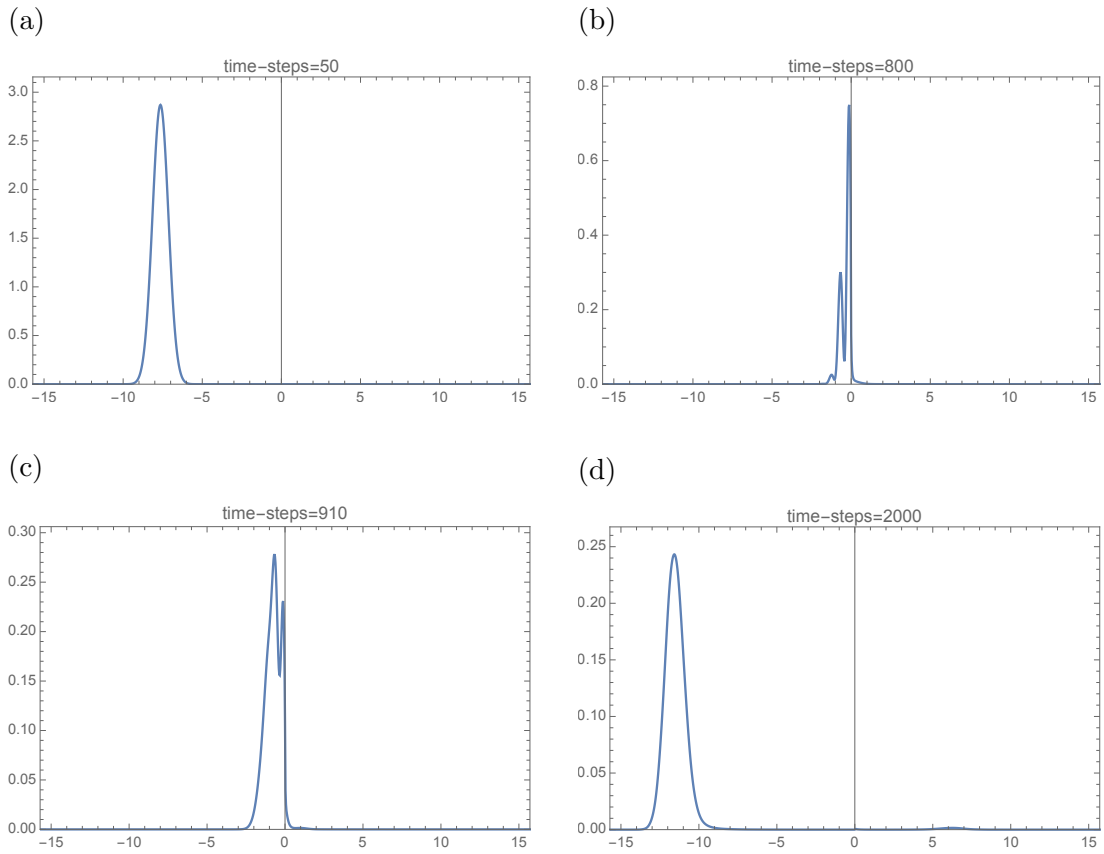

Figure 4.2: The energy density distribution of a single-photon before and after reflection by the mirrors of atoms. The initial wave packet is a Gaussian in Eq. (3.22), and here the parameters are; x0=-8.0, k_{x0} = 10.0, $\triangle^2_{kx}$=0.125, ω_j = 10.0, D_j = 4.0 and the number of modes is (N=1024). The size of the cavity is L=10π. In Fig. 4.2(a), the energy density distribution of a photon wave packet is moving towards the edges of the mirrors of atoms and reaches the mirror at Fig. 4.2(b)-(c) forming interference pattern. In Fig. 4.2(d), the wave packet is fully reflected by the mirror.

4.2 Numerical simulations of mirror and beam splitter in 1-D and 2-D

4.2.1 Mirror simulations in 1-D

We have shown how atoms can operate as a mirror for radiation. Here we show the energy density of the Hamiltonian as it moves along the x-axis. In Fig. 4.2 we present the numerical simulations of the mirror in 1-D. In the middle of the x-axis we have the atoms of the mirror. From Fig. 4.2(a), the photon is propagating towards the atoms of the mirror right at the middle. As the photon moves towards the edges of the mirror the interference pattern appears. In Fig. 4.2(d), we have shown that almost all of

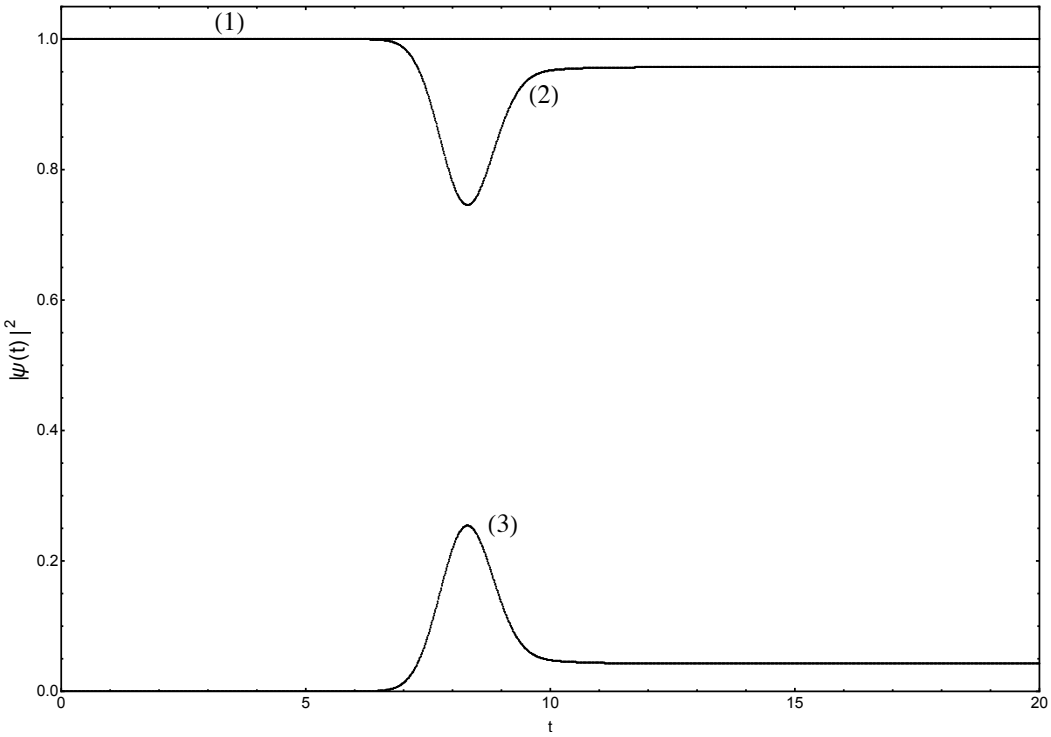

Figure 4.3: The probabilities $|\psi|^2$ of finding the field interacting with the atoms of the mirror in 1-D. Curve (1) correspond the total probability, curve (2) is the probability of the field and curve (3) is the probability of the atoms.

the radiation is being reflected by the atoms while some small portion of the radiation manages to pass through. The atoms of the mirror have seven layers, which indicate the thickness of the mirror such that it is good enough to reflect the photon.

In Fig. 4.3, we present the trace of the the probabilities $|\psi|^2$ of the field-atoms interaction in the mirror simulations in 1-D. We have labelled these probabilities as curve (1); corresponds to the probability of the total (atoms + field) interaction $|\psi_{\rm total}|^2 = |\psi_{\rm field}|^2 + |\psi_{\rm atoms}|^2$, curve (2) is for the probability of the field $|\psi_{\rm field}|^2 = \sum_k |\psi_{\rm k}|^2$ and curve (3) is for the probability of the atoms $|\psi_{\rm atoms}|^2 = \sum_j |\psi_{\rm j}|^2$ since both field and atoms are in the Fourier space. These probabilities indicate the dynamics in the simulations.

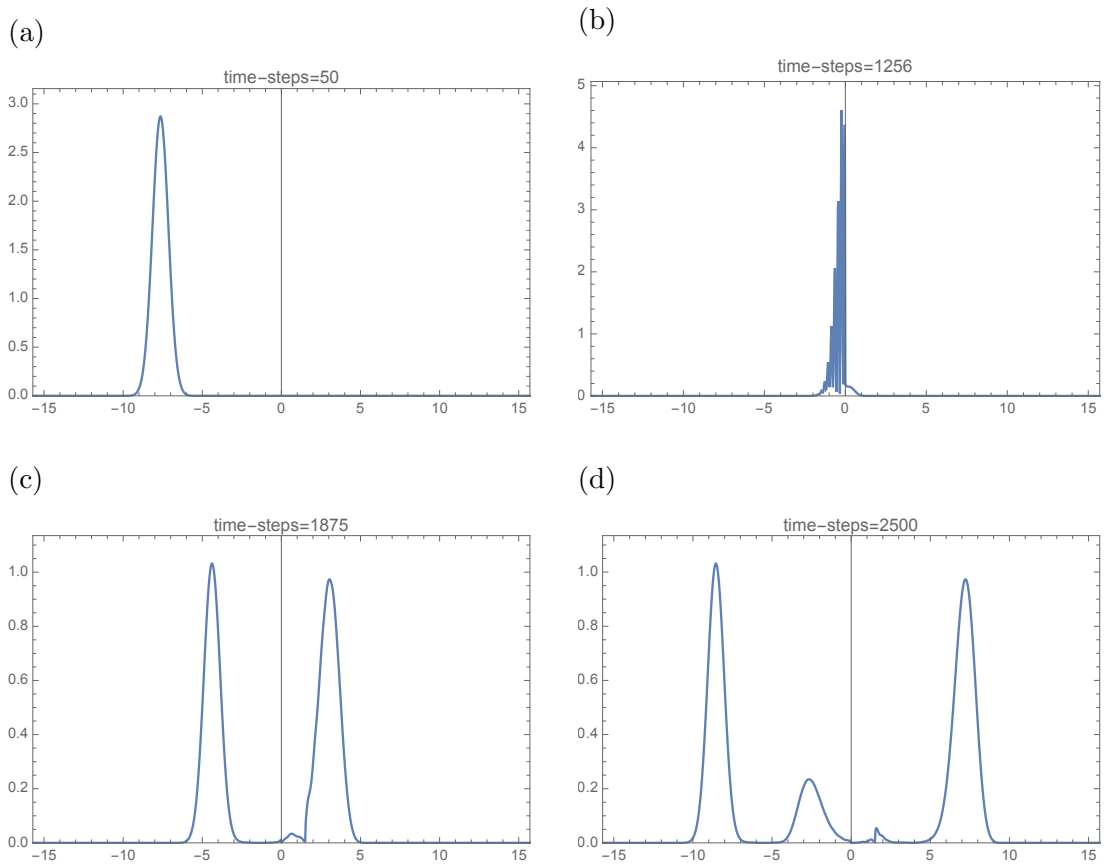

Figure 4.4: The energy density distribution of a photon before and after its gets equally divided by the beam splitter. The initial wave packet is a Gaussian in Eq. (3.22), and here the parameters are; $x0 = -8.0$, $k_{x0} = 15.0$, $\triangle_{kx}^2$=1.0, $\omega_j = 10.5$, $D_j = 6.25$ and the number of modes is (N=1024). The size of the cavity is L=10π. In Fig. 4.4(a)-(b), the energy distribution of the photon forms interference pattern as it reaches the atoms of the beam splitter and partially begins to split. In Fig. 4.4(c)-(d), the intensity of energy density distribution of a photon is being fully divided into almost two equal size by the atoms of the beam splitter.

4.2.2 A beam splitter simulations in 1-D

We have shown that it is possible for a beam splitter to be built by atoms. In order for us to carry out this simulation we had to reduce the number of layers of the atoms to one that is the thickness of the atoms. In Fig. 4.4, we present the numerical simulations of the beam splitter in 1-D. In the centre of the x-axis we have the atoms of the beam splitter. In Fig. 4.4(a), we have a photon moving towards the edges of the atoms of the beam splitter. As the photon reaches the beam splitter, there is an interference structure. In Fig. 4.4(d), almost half of the radiation is reflected back by the atoms and the remaining part is transmitted as it is shown. In Fig. 4.5,

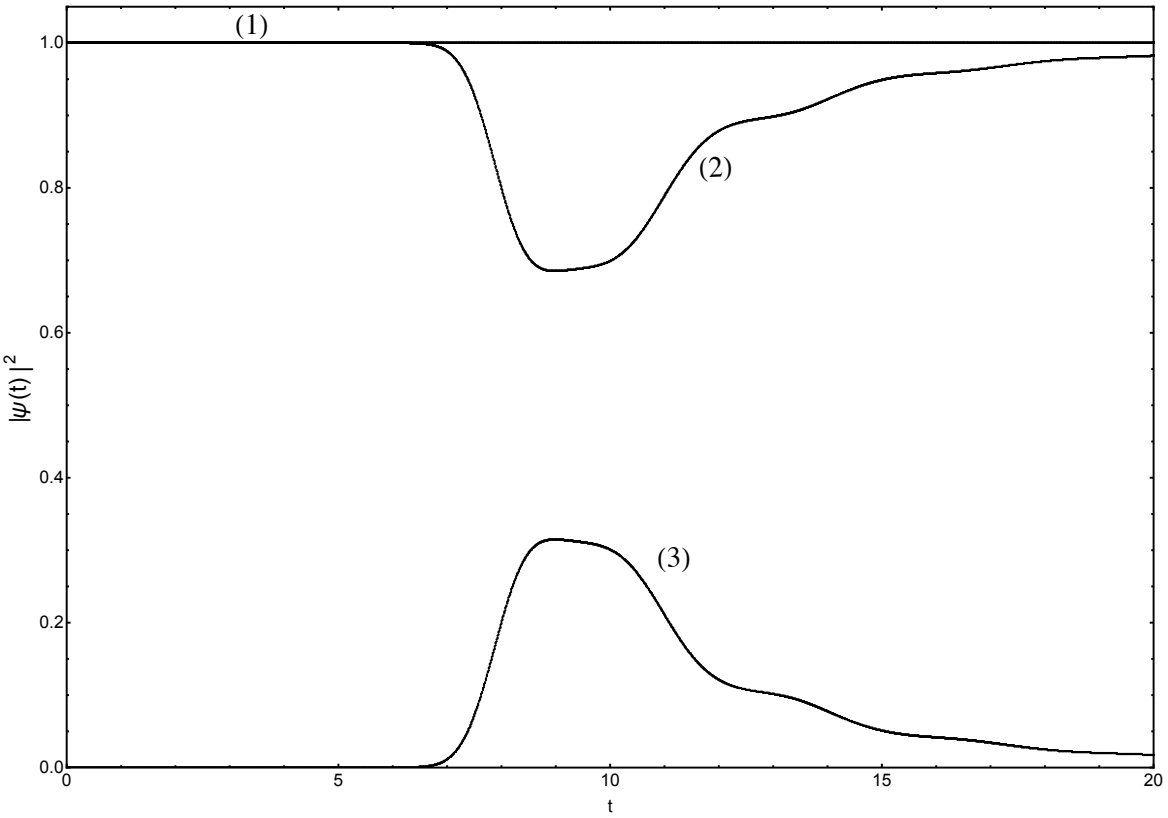

Figure 4.5: The probabilities $|\psi|^2$ of finding the field interacting with the atoms of the beam splitter in 1-D. Curve (1) correspond the total probability, curve (2) is the probability of the field and curve (3) is the probability of the atoms.

we present the trace of the the probabilities $|\psi|^2$ of the light atoms interaction. We have labelled these probabilities as follows; curve (1) denote the probability of the total (atoms + field) interaction $|\psi_{\text{total}}|^2 = |\psi_{\text{field}}|^2 + |\psi_{\text{atoms}}|^2$, curve (2) is for the probability of the field $|\psi_{\text{field}}|^2 = \sum_k |\psi_{\text{k}}|^2$ and curve (3) is for the probability of the atoms $|\psi_{\text{atoms}}|^2 = \sum_j |\psi_{\text{j}}|^2$ since both field and atoms are in the Fourier space. These probabilities presents the behaviour of the norm in the beam splitter simulation as we can see in Fig. 4.5 that the total probability gives us 1, which confirms that there is dynamic in the simulation. In the next sections, we switch to 2-D and conduct the numerical simulations of both mirror and beam splitter, respectively.

4.2.3 Mirror simulations in 2-D

We have shown that it is possible for atoms to reflect and transmit the radiation of the photon in 1-D above. Here we want to switch to 2-D and perhaps apply the same

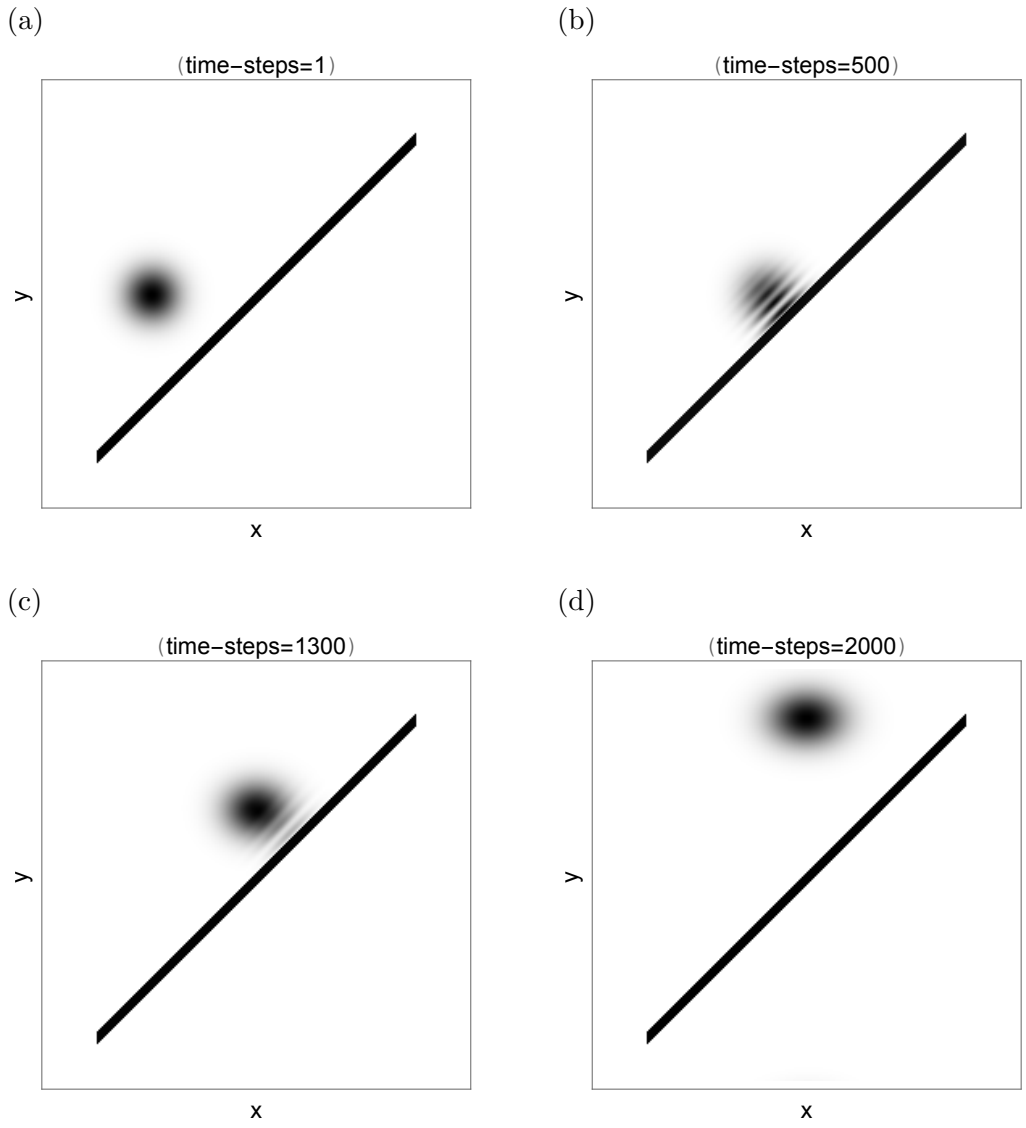

Figure 4.6: The energy density distribution of a single-photon before and after being reflected by the mirrors of atoms. The initial wave packet is a Gaussian in Eq. (3.22) and the parameters are the same to that of the free-photon simulation given in Fig. 4.1, respectively. In Fig. 4.6(a), the energy density distribution of the incoming photon is approaching the mirror. As it reaches the mirror in Fig. 4.6(b) the incoming photon interferes with the re-emitted radiation. In Fig. 4.6(c) the interference pattern occurs as the photon gets partially reflected by the mirror. In Fig. 4.6(d), the energy density of the photon wave packet is being fully reflected by the mirrors of atoms.

procedure to produce these simulations. In Fig. 4.6, we have the atoms of the mirror arranged into an elongated atomic slab positioned at the centre of the cavity at angle of 45 degrees. There are seven layers of the atoms. In Fig. 4.6(a) we have a photon propagating towards the atoms. As the photon reaches the atoms, almost all of the intensity is being partially reflected in Fig. 4.6(b)-(c). As a result, we can see the

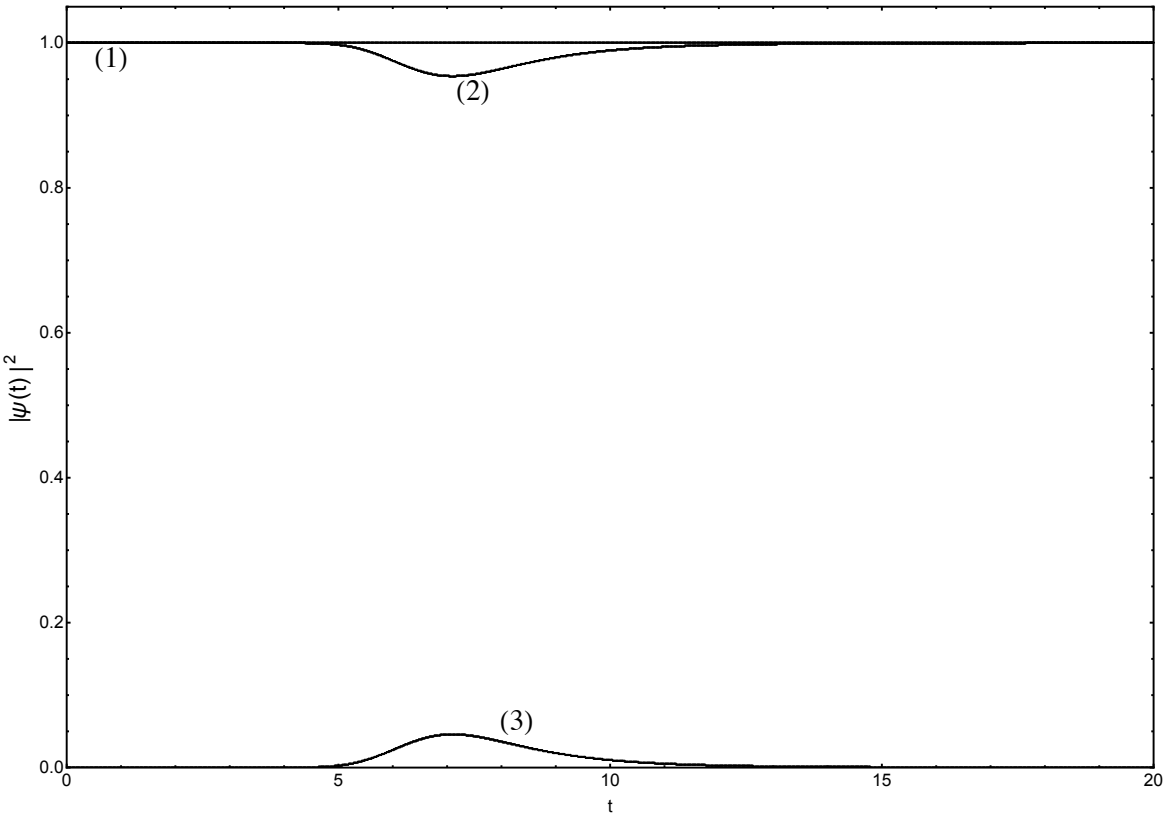

Figure 4.7: The probabilities $|\psi|^2$ of the field and atoms of the mirror in 2-D. Curve (1) correspond the total probability, curve (2) is the probability of the field and curve (3) is the probability of the atoms.

interference structure when the incoming and the reflected radiation interferes. In Fig. 4.6(d), the atoms of the mirror fully reflect photon making sure that no portion of the radiation passes through the mirror. The intensity profile of the radiation that is fully reflected is no longer symmetric.

In Fig. 4.7, we present the plot of the trace of the the probabilities $|\psi|^2$ of the light atoms interaction in the mirror simulations. We have labelled these probabilities as follows; curve (1) presents the time dependent of numerical calculations of $|\psi|^2$ as we can see that the total probability gives us 1, curve (2) corresponds to the probability of the field and curve (3) corresponds to the probability of the atoms since both field and atoms are in the Fourier space. These probabilities confirms that there is dynamic in the simulations as we can clearly see how the energy that goes into the mirror and gets reflected. The shape of curve (2) and curve (3) shows that, there is some interaction between the atoms and the light and the probability of finding excitation in light is decreasing while in the same way it is increasing in the atoms and afterwards the excitation goes to the atoms and gets reflected back.

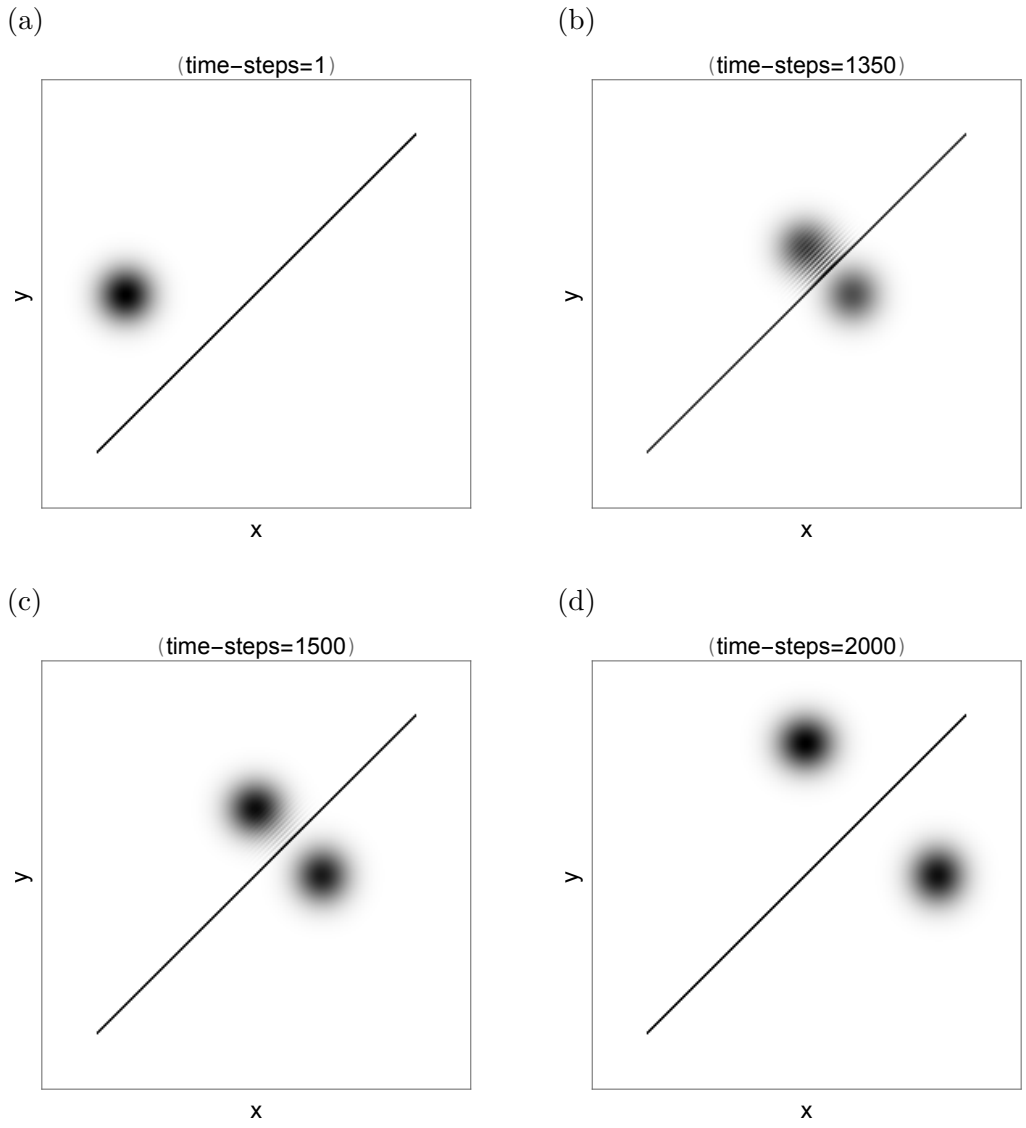

Figure 4.8: The energy density distribution of a photon wave packet before and after being equally divided by the atoms of the beam splitter. The initial Gaussian wave packet is given in Eq. (3.22), with the parameters; x0=-10.0, y0=0.0, k_{x0} = 15.0, k_{y0} = 0, $\triangle_{kx}^2$=$\triangle_{ky}^2$=0.125, ω_j = 10.4, D_j = 0.5 and the number of modes is (N=256). The size of the cavity is L=10π. In Fig. 4.8(a), the energy density distribution of a photon wave packet is coming towards the beam splitter. In Fig. 4.8(b)-(c), the photon is partially divided into two halves by the beam splitter as we can see the interference structure which shows part of the radiation being transmitted. In Fig. 4.8(d), the photon is being fully equally divided by the atoms of beam splitter.

4.2.4 A beam splitter simulations in 2-D

In this simulation, we demonstrate that it is possible to simulate the beam splitter provided that we reduce the number of layers of the atoms in the centre. In Fig. 4.8, we present the numerical simulations of the beam splitter in 2-D. In Fig. 4.8(a), it

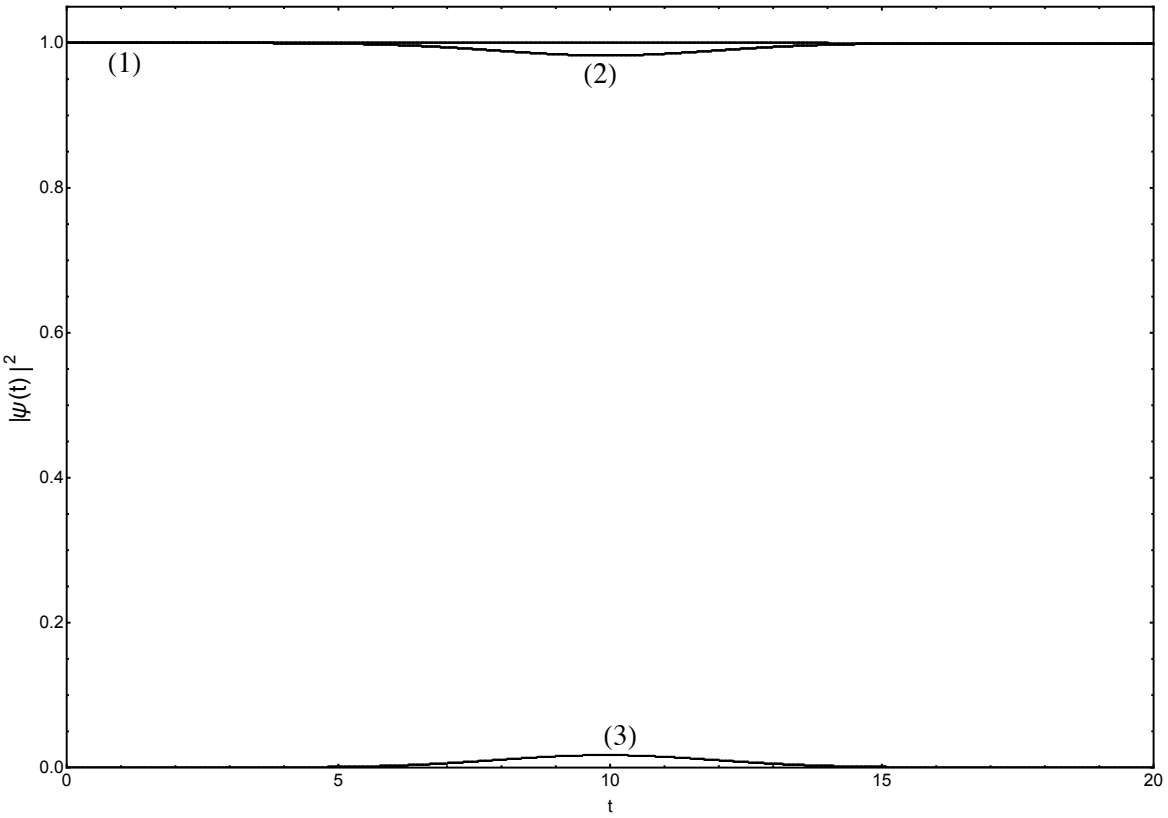

Figure 4.9: The probabilities $|\psi|^2$ of the field and atoms of the beam splitter in 2-D. Curve (1) correspond the total probability, curve (2) is the probability of the field and curve (3) is the probability of the atoms.

is clearly seen as the photon approaches the atoms of the beam splitter. As can be seen in Fig. 4.8(b)-(c), on the left of the atoms of the beam splitter we have the interference pattern whereas on the right we have the outgoing part of radiation with no interference. In Fig. 4.8(d), part of the photon wave packet is being reflected by the atoms of the beam splitter and the remaining part manages to pass through the single layer atoms.

We can then concede that, the photon excites the atoms and this imply the quantum interference between incoming photon and the emitted photon such that almost half of the original radiation gets transmitted by the atoms and the rest of the radiation is being reflected. In essence, the incoming photon is split into two equal halves with one moving up and the other one moving to the right. Essential, we can see that the atoms in such a case forms a 50:50 beam splitter for the incoming radiation. This implies that, the quantum beam splitter and mirror are linear devices and this is important if one want to build optical networks out of the considered optical elements.

In Fig. 4.9, we present the plot of the trace of the the probabilities $|\psi|^2$ of the light atoms interaction. We have labelled these probabilities as follows; curve (1) presents the time dependent of numerical calculations of $|\psi|^2$ and the total probability gives us 1, curve (2) corresponds to the probability of the field and curve (3) corresponds to the probability of the atoms since both field and atoms are in the Fourier space. These probabilities presents how the norm behaves in the beam splitter simulation which serves as a proof that there is dynamics in the simulation. From the function, we can clearly see how the energy that goes into the beam splitter is being transmitted and reflected equally. The shape of curve (2) and curve (3) indicate the interaction between the light and the atoms of the beam splitter, which implies that, there is 50:50 probability of getting excitation in the light since it is decreasing and slightly increasing in the atoms, respectively.

We investigated in the thesis, an approach that offers a direct quantum-mechanical way to simulate more complex optical elements, and that is exactly what we plan to build in future, i.e; the optical polarizer beam splitter, wave plates, dove prisms etc. In general, these optical components are considered to be classical objects in the description of propagation, scattering, reflected and transmitted wave. In this work, we modelled the full system quantum mechanically and surprisingly the transmitted and reflected wave occurs naturally as a result of quantum-mechanical interference. This direct numerical simulation, allows us to create a new optical setup with multiple components where we will consider the behaviour of the system to be derived from the first principles of quantum mechanics. These QED simulations also offers us an opportunity to build cavities of arbitrary shape and analyse the time evolution of the photon intensity inside the cavity. Furthermore, another possibility would be to conduct direct simulations with atoms moving inside the cavity, and consider the basis states to have more than one photon excitation.

Chapter 5

Conclusions

In this work, we have numerically studied a quantum electrodynamic model to describe light-matter interactions at a fundamental level. We have demonstrated the numerical simulations to illustrate how a two-level systems interacts with the quantized field inside a two dimensional cavity. All the numerical simulations were done in both 1-D and 2-D, respectively. This model enables us to understand, at the microscopic levels how a photon wave packets propagates through an arrangement of a crystal grid of atoms. In addition the model allows us to formulate another way to generalise the system, like extending our work into the 3 dimension. In the 3-D case we can conduct more interesting simulations, such as the microscopic simulation of a QKD Protocol. Also, one could generalise the model by increasing the number of excitations together with the number of levels.

Bibliography

[1] Claude Cohen-Tannoudji, Jacques Dupont-Roc, Gilbert Grynberg, and Patricia Thickstun. *Atom-photon interactions: basic processes and applications*. Wiley Online Library, 1992.

[2] Peter W Milonni. *The quantum vacuum: an introduction to quantum electrodynamics*. Academic press, 2013.

[3] Nathan D Poulin. A quick introduction to the strong coupling regime of cavity quantum electrodynamics: applications and fundamental quantum theory. *arXiv preprint arXiv:1412.0335*, 2014.

[4] E Vetsch, D Reitz, G Sagué, R Schmidt, ST Dawkins, and A Rauschenbeutel. Optical interface created by laser-cooled atoms trapped in the evanescent field surrounding an optical nanofiber. *Physical review letters*, 104(20):203603, 2010.

[5] Manoj Das, A Shirasaki, KP Nayak, M Morinaga, Fam Le Kien, and K Hakuta. Measurement of fluorescence emission spectrum of few strongly driven atoms using an optical nanofiber. *Optics express*, 18(16):17154–17164, 2010.

[6] Laura Russell, Kieran Deasy, Mark J Daly, Michael J Morrissey, and Síle Nic Chormaic. Sub-doppler temperature measurements of laser-cooled atoms using optical nanofibres. *Measurement Science and Technology*, 23(1):015201, 2011.

[7] A Goban, KS Choi, DJ Alton, D Ding, C Lacroûte, M Pototschnig, T Thiele, NP Stern, and HJ Kimble. Demonstration of a state-insensitive, compensated nanofiber trap. *Physical Review Letters*, 109(3):033603, 2012.

[8] Michael J Morrissey, Kieran Deasy, Mary Frawley, Ravi Kumar, Eugen Prel, Laura Russell, Viet Giang Truong, and Síle Nic Chormaic. Spectroscopy, ma-

nipulation and trapping of neutral atoms, molecules, and other particles using optical nanofibers: a review. *Sensors*, 13(8):10449–10481, 2013.

[9] Edwin T Jaynes and Frederick W Cummings. Comparison of quantum and semi-classical radiation theories with application to the beam maser. *Proceedings of the IEEE*, 51(1):89–109, 1963.

[10] W Neuhauser, M Hohenstatt, P Toschek, and H Dehmelt. Optical-sideband cooling of visible atom cloud confined in parabolic well. *Physical Review Letters*, 41 (4):233, 1978.

[11] David J Wineland, Robert E Drullinger, and Fred L Walls. Radiation-pressure cooling of bound resonant absorbers. *Physical Review Letters*, 40(25):1639, 1978.

[12] Arthur Ashkin. Optical trapping and manipulation of neutral particles using lasers. *Proceedings of the National Academy of Sciences*, 94(10):4853–4860, 1997.

[13] M Havukainen, G Drobnỳ, S Stenholm, and V Bužek. Quantum simulations of optical systems. *journal of modern optics*, 46(9):1343–1367, 1999.

[14] Rodney Loudon and Thomas von Foerster. The quantum theory of light. *American Journal of Physics*, 42(11):1041–1042, 1974.

[15] Daniel F Walls and Gerard J Milburn. *Quantum optics*. Springer Science & Business Media, 2007.

[16] Mark Fox. *Quantum optics: an introduction*, volume 15. OUP Oxford, 2006.

[17] Leonard Mandel and Emil Wolf. *Optical coherence and quantum optics*. Cambridge university press, 1995.

[18] Mark Beck. Introductory quantum optics.. *American Journal of Physics*, 73(12): 1197–1198, 2005.

[19] Stig Stenholm. Quantum theory of electromagnetic fields interacting with atoms and molecules. *Physics Reports*, 6(1):1–121, 1973.

[20] Marlan O Scully and M Suhail Zubairy. *Quantum optics*. Cambridge university press, 1997.

[21] John Weiner and P-T Ho. *Light-matter interaction, Fundamentals and applications*, volume 1. John Wiley & Sons, 2008.

[22] WH Press, SA Teukolsky, WT Vetterling, and BP Flannery. Numerical recipes in c, 2nd edit. *Cambridge University, New York*, 1992.